IMPACT OF CATALYST COMPOSITION ON OLEFIN AROMATIZATION IN PRESENCE AND ABSENCE OF HYDROGEN

by

Christopher K. Russell

A Dissertation

Submitted to the Faculty of Purdue University

In Partial Fulfillment of the Requirements for the degree of

Doctor of Philosophy

Davidson School of Chemical Engineering

West Lafayette, Indiana

August 2023

THE PURDUE UNIVERSITY GRADUATE SCHOOL
STATEMENT OF COMMITTEE APPROVAL

Dr. Jeffrey T. Miller, Chair

Davidson School of Chemical Engineering

Dr. Rajamani Gounder

Davidson School of Chemical Engineering

Dr. Jeffrey P. Greeley

Davidson School of Chemical Engineering

D. Abhaya K. Datye

Chemical & Biological Engineering

University of New Mexico

Approved by:

Dr. John Morgan

Dedicated to my family, friends, and future students.

ACKNOWLEDGMENTS

First and foremost, I would like to thank my advisor, Jeff Miller, for the guidance and support he has demonstrated throughout my time at Purdue. Second, I would like to thank my committee, Dr.s Rajamani Gounder, Jeffrey P. Greeley, and Abahya K. Datye for the insightful questions and feedback helping me develop as a researcher. I would like to thank my fellow Ph.D students, M.S. students, undergraduate researchers, and visiting scholars in the Miller Group for their training, intellectual discussion, support, and encouragement throughout my Ph.D.

Additionally, I would like to thank the professors of the various classes I worked as a Teaching Assistant: Dr. Stephen Beaudoin, Dr. Raj Gounder, Dr. Sangtae Kim, Dr. Johannes Nitsche, and AraOluwa Adaramola. Their dedication to their classes has inspired me to pursue a career in teaching, and the experience I have gained working with students has been invaluable in preparing me for future classes.

I acknowledge the financial support for this study from the National Science Foundation under Cooperative Agreement No. EEC-1647722, an Engineering Research Center for the Innovative and Strategic Transformation of Alkane Resources. The XAS measurements in this research used resources at the 8-ID Beamline of the National Synchrotron Light Source II, a US Department of Energy (DOE) Office of Science User Facility operated by Brookhaven National Laboratory under contract number DE-SC0012704, and those of the Advanced Photon Source, a US DOE Office of Science User Facility operated for the DOE Office of Science by Argonne National Laboratory under contract number DE-AC02-06CH11357.

TABLE OF CONTENTS

LIST OF TABLES

LIST OF FIGURES

ABSTRACT

The expanded production of shale gas has increased the desire for developing methods for converting light alkanes, especially propane and ethane, into aromatic species (i.e., benzene, toluene, and xylene). A multi-step process for conversion of light alkanes to aromatics may be developed, where the first stage converts light alkanes into olefins and hydrogen, and the second stage converts olefins to aromatics. However, to determine the viability of this process, better understanding of the performance of olefin aromatization in the presence of equimolar hydrogen is necessary.

Previous studies on the conversion of olefins to aromatics with bifunctional ZSM-5 catalysts have concluded that benzene, toluene, and xylenes (BTX) yields are significantly higher than for ZSM-5 alone. These results were attributed to the presence of a dehydrogenation function of Ga or Zn leading to higher rates of aromatics formation. In this study, a highly active, bifunctional $PtZn/SiO_2$ (1.3 wt% Pt, 2.6 wt% Zn) with H-ZSM-5 (Si/Al = 40) catalyst is investigated for propene aromatization at 723 K and 823 K. At low to moderate propene conversions, in addition to BTX, light alkanes and olefins are produced. Many of these may also be converted to aromatics at higher propene conversion while others are not, for example, light alkanes. When compared at equivalent space velocity and propylene conversion, the bifunctional catalyst has a much higher selectivity to aromatics than ZSM-5; however, when compared at equivalent conversion of all reactive intermediates, the bifunctional catalyst exhibits very similar BTX selectivity. At 723 K, for both ZSM-5 and the bifunctional catalyst, the primary non-reactive by-products are propane and butane. At 823 K, both ZSM-5 and the bifunctional catalyst convert propane and butane to aromatics increasing the aromatic yields, and the by-products are methane and ethane.

Additionally, previous studies have investigated the H-ZSM-5 and Ga/H-ZSM-5 in the absence of H_2, which is necessary to understand in order to develop a process for the conversion of light alkanes to aromatics. Herein, proton-form ZSM-5 and Ga modified H-ZSM-5 are compared for propylene aromatization in the presence and absence of equimolar hydrogen at 1.9 kPa and 50 kPa partial pressures. At 1.9 kPa, the presence of H_2 is shown to have no impact on the product distribution on H-ZSM-5 or Ga/H-ZSM-5. At 50 kPa, H_2 is shown to have no significant impact on H-ZSM-5 and has no impact on Ga/H-ZSM-5 at conversions <80%. Additionally, the

addition of Ga to H-ZSM-5 is shown to have no impact on the product distribution in the presence or absence of H_2, contrary to previous reports. The disagreement with previous literature stems from previous literature comparing H-ZSM-5 and Ga/H-ZSM-5 at equivalent space velocity rather than equivalent propylene conversion despite previous studies showing that the presence of Ga increases the conversion at equivalent space velocity for olefin aromatization.

1. INTRODUCTION

Light gaseous hydrocarbons have become more available in the US because of the development in technologies such as hydraulic fracturing and horizontal drilling to harvest abundant shale gas reserves.[1] Shale gas consists largely of methane, ethane, propane, and butane, which can be converted to light alkenes (ethene, propene) via cracking [2–7] or dehydrogenation reactions.[1,6,8–11] The conversion of short-chain alkenes to valuable aromatic hydrocarbons, such as benzene, toluene, and xylenes (BTX) and high-octane gasoline has been of interest over the last decades.[10,12–15] While industrial processes for conversion of large alkanes (i.e., butane and larger hydrocarbons) have been reported, they remain inadequate for the conversion of light alkanes (i.e., ethane and propane). One potential process for the conversion of light alkanes to aromatics involves two steps. First, alkanes are converted to olefins, which may be done via catalytic dehydrogenation or via cracking reactions. In the second stage, olefins may be converted to aromatics. This work focuses on the second step: olefin conversion, using propylene as a model species for investigating olefin aromatization.

Propylene aromatization is generally done using bifunctional metal-acid catalysts. Proton form zeolite ZSM-5 (H-ZSM-5) is typically used as the acid function due to its higher stability compared to other zeolite-type catalysts. Studies on H-ZSM-5 have achieved between 25 – 45% BTX selectivity at temperatures above 573 K, compared to selectivities around 70% when bifunctional metal-acid catalysts (i.e., Ga/H-ZSM-5 or Zn/H-ZSM-5) are used [16–18]. However, these studies compare product distributions at equivalent space velocity rather than at equivalent reaction conversion. For example, Shibata and co-workers report 40% selectivity to aromatics at 10 g h mol^{-1} compared to 75% on Ga/H-ZSM-5 [17]. However, the conversion on H-ZSM-5 was 80% compared to near 100% conversion on Ga/H-ZSM-5.

The differences in aromatic selectivity at equivalent space velocity have been attributed to the metal function acting as a dehydrogenation function. Lechert and co-workers measured the molar ratio of alkanes to aromatics for aromatization on H-ZSM-5 and Ga/H-ZSM-5 to be 2.9 and 0.9, respectively [16]. The lower ratio in the presence of Ga suggests that Ga enables catalytic dehydrogenation of cyclic hydrocarbons to form aromatic rings, whereas Brønsted acid protons follow cracking mechanisms, generating 3 alkanes per aromatic. In addition to increasing the

selectivity to aromatics via enabling a dehydrogenation mechanism, the presence of Ga has also been shown to increase the rate of propene conversion to aromatics.

The presence of Ga has been shown to significantly increase the propene conversion at equivalent space velocity. This implies that, in addition to increasing aromatic selectivity, the rate of aromatics conversion is also improved. Isotopic kinetic studies by Iglesia and Biscardi confirm this notion, finding that the presence of Ga increases the rate of propene conversion to aromatics by a factor of 4 compared to solely H-ZSM-5 [19]. In short, the presence of Ga has been reported to increase both the rate and selectivity of propene aromatization due to Ga enabling dehydrogenation of alkanes enabling an alternative mechanism for aromatization reactions to occur. However, there are a few primary shortcomings in studies of olefin aromatization. Firstly, studies have compared product distributions at equivalent space velocity, rather than at equivalent conversion. Thus, differences in reaction progress potentially lead to apparent differences in product distributions. Secondly, studies of olefin conversion have been conducted in the absence of hydrogen. The first step of the conversion of alkane to aromatics converts alkanes to olefins and hydrogen. The separation of hydrogen from olefins is an expensive process requiring cryogenic distillation. Thus, it is necessary to understand the effects of propylene aromatization in the presence of equimolar hydrogen, which would be produced from the conversion of alkanes to olefins. These two shortcomings are the topic of this thesis.

In Chapter 2, the effect of dehydrogenation reactivity on the propylene aromatization product distribution is investigated. Results indicating that the presence of a dehydrogenation function increasing aromatics selectivity and rate suggests that using a more reactive dehydrogenation catalyst (i.e., PtZn nanoparticles) will further enhance the aromatics selectivity. In this study, PtZn nanoparticles supported on SiO_2 are physically mixed with H-ZSM-5, and the product distribution is measured. When comparing product distributions at equivalent propylene conversion at equivalent propylene conversion, PtZn increases aromatic selectivity compared to H-ZSM-5, similar to previous studies with Ga, for example. However, it is noted that the other products formed are predominantly alkenes that are reactive for aromatization in and of themselves. Thus, in terms of developing a process for converting propylene to aromatics and high-octane gasoline, these products would be recycled and further reacted to form aromatics. When comparing product distributions in terms of all species that react to form aromatics, the product distribution on H-ZSM-5 and PtZn/H-ZSM-5 are very similar. Further, this study shows that at 723 K, methane,

ethane, propane, and butane are stable products on H-ZSM-5, whereas methane, ethane, and propane are stable products on PtZn/H-ZSM-5. At 823 K, propane and butane become reactive on H-ZSM-5 and PtZn/H-ZSM-5. The difference in aromatic selectivity observed at the higher temperature is due to propane and butane becoming reactive at the elevated temperature.

In Chapter 3, the effect of hydrogen on the product distribution of propylene aromatization is investigated on Ga/H-ZSM-5 and on H-ZSM-5 at 2.9 kPa and 50 kPa. At 2.9 kPa, the presence of H_2 has no impact on the product distribution of propylene aromatization on H-ZSM-5 or on Ga/H-ZSM-5. At 50 kPa and propylene conversions above 80%, H_2 increases the selectivity to butane and slightly decreases the selectivity to aromatics. However, at low and intermediate conversions, H_2 does not change the product distribution. The product distribution is shown to also be affected by the partial pressure of the reactants, where at lower partial pressures (i.e., 2.9 kPa), aromatics are favored, whereas at higher partial pressures, non-aromatic products are favored.

Chapter 4 provides overall conclusions of the studies and recommendations for further development of a process for converting light alkanes to aromatics via dehydrogenation and subsequent aromatization of olefins is provided. Collaboration with process optimization studies (i.e., Thrust 4 in CISTAR) and economic analysis is suggested to determine the optimal operating pressure, temperature, extent of hydrogen separation (if any) and investigate the economic viability of a process for the conversion of light alkanes to aromatics via sequential dehydrogenation and aromatization. Additionally, studying the effect of hydrogen on the stability of aromatization catalysts is recommended as a future area of study.

2. INFLUENCE OF BIFUNCTIONAL PTZN/SIO_2 AND H-ZSM-5 ON THE RATES AND SELECTIVITY OF PROPENE AROMATIZATION

Submitted to Zeolite Materials and Catalysis

2.1 Introduction

Advances in mining and extraction techniques such as hydraulic fracturing and horizontal drilling have led to an abundance of light hydrocarbons from shale formations [1]. Shale gas consists mainly of methane, ethane, propane, and butane. The natural gas liquids can be converted to light alkenes via dehydrogenation [1,6,8–11] or cracking [2,3,5–7], which can be further converted to valuable aromatic hydrocarbons, such as benzene, toluene, xylenes (BTX), and high-octane gasoline [13–16,20].

Alkene aromatization reactions are generally catalyzed using ZSM-5 at higher temperatures and lower pressures [18,21,22]. For example, propylene aromatization by H-ZSM-5 (Si/Al = 50-100) at 523 K - 850 K gives low selectivity to aromatic products (~35%) and high selectivity to low value light paraffins (~60%); while with higher Si/Al ratios (from 140 – 500) at 573 K trace amounts of aromatics were observed [16]. Similar aromatic yields were observed by Norval and co-workers for propene, 1-butene, and 2-methylpropene conversion over H-ZSM-5 at 663 – 773 K [23]. The mechanism for acid catalyzed olefin aromatization was proposed by M.L. Poutsma in 1976, suggesting that aromatic molecules are formed from olefins via successive deprotonation and hydride transfer to carbenium ions [24]. Here, the formation of one aromatic molecule also forms three paraffin molecules, i.e., alkane/aromatic mole ratio = 3. Ono and co-workers confirmed the validity of this mechanism on H-ZSM-5 for butene aromatization at 773 K, reporting an alkane/aromatic molar ratio = 2.9, consistent with this mechanism [18].

Using bifunctional catalysts having both Brønsted acid sites (H+) and a dehydrogenation function (e.g., Ga [11,17,18,25], Zn [11,16], or Cu [22,26]), the aromatic selectivity can be increased to about 70%. The other by-products were methane, ethane, ethene, propane, butenes, and C_{5+} olefins. For bifunctional catalysts the alkane/aromatic mole ratio decreases to less than 1, suggesting that aromatics are formed by a different mechanism, i.e., dehydrogenation on Zn or Ga [11,17,18,26].

While metallic Pt has a much higher rate for dehydrogenation than Ga or Zn oxides, Pt is highly selective to methane by hydrogenolysis giving low aromatic yields. In addition, Pt nano-particles form coke and rapidly deactivate ZSM-5 [27]. However, intermetallic alloys of Pt, for example, Pt_1Zn_1, minimize methane and coke formation and have significantly improved deactivation stability [28]. In this study, bifunctional (PtZn/SiO2 + H-ZSM-5) catalysts are compared to H-ZSM-5 for propene aromatization at 723 and 823 K. This study demonstrates that bifunctional H-ZSM-5 catalysts do increase the aromatic selectivity when compared at constant propylene conversion or reaction conditions [11,17,18,21], but do not increase the aromatic selectivity, when compared at conversion of all reactive intermediates. The unreactive alkane products, i.e., methane, ethane, propane and butane, also differ depending on the reaction temperature.

2.2 Materials and Methods

Commercial ammonium form ZSM-5 (NH_4-ZSM-5, Zeolyst International, CBV 8014, Si/Al=40) was first calcined at 773 K for 3 h (5°C/min ramp rate) to convert to the acidic form of ZSM-5 (H-ZSM-5). The H-ZSM-5 was then pelletized to 35 - 50 mesh (similar size to the $PtZn/SiO_2$).

$PtZn/SiO_2$ was synthesized similar to previously reported methods [2,29]. First, Zn is deposited on silica (SiO_2; Davisil Grade 646, Sigma Aldrich, 35 - 60 mesh) using strong electrostatic adsorption of Zn^{+2} ions. To prepare 5 g $PtZn/SiO_2$, 0.68 g zinc nitrate hexahydrate ($Zn(NO_3)_2{\cdot}6H_2O$, Sigma Aldrich) was dissolved in approximately 50 mL Millipore water. Concentrated ammonium hydroxide was then added to the solution until pH>11. The 5 g SiO_2 was added to the Zn solution and stirred using a Teflon stir bar for 10 minutes. The suspended SiO_2 was filtered and washed with 50 mL Millipore water three times before drying overnight at 398 K in stagnant air. Subsequently, it was calcined at 573 K for 3 h (10°C/min), yielding approximately 3 wt % Zn on silica (Zn/SiO_2).

Pt was added to the Zn/SiO_2 by incipient wetness impregnation. Its pore volume was determined by adding Millipore water dropwise until visibly saturated (measured to be 1.0 mL/g SiO_2). The Pt impregnation solution was prepared by dissolving 0.2 g tetraamine platinum (II) nitrate ($Pt(NH_3)_4(NO_3)_2$, Sigma Aldrich) in 2 mL Millipore water. Concentrated NH_4OH was then added to the solution until pH>11, approximately 1.5 mL. Millipore water was added to the

solution to yield 5 mL total solution volume. The solution was then added dropwise to the Zn/SiO_2 while stirring until the entire solution was consumed. The Pt-impregnated Zn/SiO_2 was then dried overnight at 398 K in stagnant air and calcined at 473 K for 3 h (5°C/min ramp rate) before being reduced at 498 K under flowing 5% H_2 (balance N_2, 100 cm^3/min). To confirm Pt_1Zn_1 intermetallic alloy was synthesized, the catalyst was tested for propane dehydrogenation to ensure >97% propylene selectivity at 823 K.

Elemental analysis of the $PtZn/SiO_2$ catalyst was determined using Inductive Coupled Plasma-Optical Emission Spectrometry (ICP-OES) measurements performed on a Thermo Scientific iCAP 7000 Plus Series spectrometer. Preparation involved digestion of 0.272 g of sample with 2.07 g HF (Sigma Aldrich, 48%) for 48 h, then dilution with 49.5 g of deionized water. After digestion and dilution, a 2.14 g aliquot was removed and mixed with 0.54 g of HNO_3 (Sigma Aldrich, 70%). Calibration standards were prepared by diluting stock standard solutions of Pt, Zn, Al, and Si (Sigma Aldrich). The concentration of Pt and Zn was measured to be 1.3% and 2.6%, respectively.

The bifunctional catalyst was prepared to give a 1:1 mass ratio of $PtZn/SiO_2$ and H-ZSM-5. Catalyst weights from 0.005 - 1 g were diluted to a total sample bed mass of 1 g using SiO_2. The sample mixture was then loaded into a 10 mm I.D. quartz tube, using quartz wool to support the catalyst with an internal thermocouple monitoring the temperature of the catalyst bed. The quartz reactor was loaded into a vertically aligned clamshell furnace. The catalyst was heated to approximately 373 K while flowing 100 cm^3/min N_2 and held for 15 minutes before heating to the reaction temperature (723 - 823 K) in flowing N_2. After reaching the reaction temperature, a flow of 100 cm^3/min 5% H_2 (balance N_2, Indiana Oxygen) for 30 minutes reduced the catalyst forming the PtZn alloy. The reaction is then initiated by flowing 100 cm^3/min 3% C_3H_6 (balance N_2, Indiana Oxygen) over the catalyst bed. Cyclohexene catalytic conversion was performed by bubbling 10 - 100 cm^3/min N_2 through cyclohexene (Sigma Aldrich, 99%). Products were analyzed using a Hewlett Packard 7890 gas chromatograph with an Agilent HP/AL-S column and a flame ionization detector.

2.3 Results

2.3.1 H-ZSM-5 catalyzed propene aromatization product distribution

As shown in Figure 2.1, reaction products on H-ZSM-5 include light alkanes, (methane, ethane, propane, butane), olefins (ethylene, butenes, pentenes and hexenes) and aromatics (benzene, toluene and xylenes). At 723 K, the selectivity of CH_4 and C_2H_6 increases with increasing propene conversion (Figure 2.1a); however, the carbon selectivity of both remains low at all conversions (<2%). The propane carbon selectivity increases from about 5% to 22% as the propene conversion increases from 30 to 85%. The carbon selectivity of butane also increases, from 0.5% to 17%, at propene conversions from 4% to 85%.

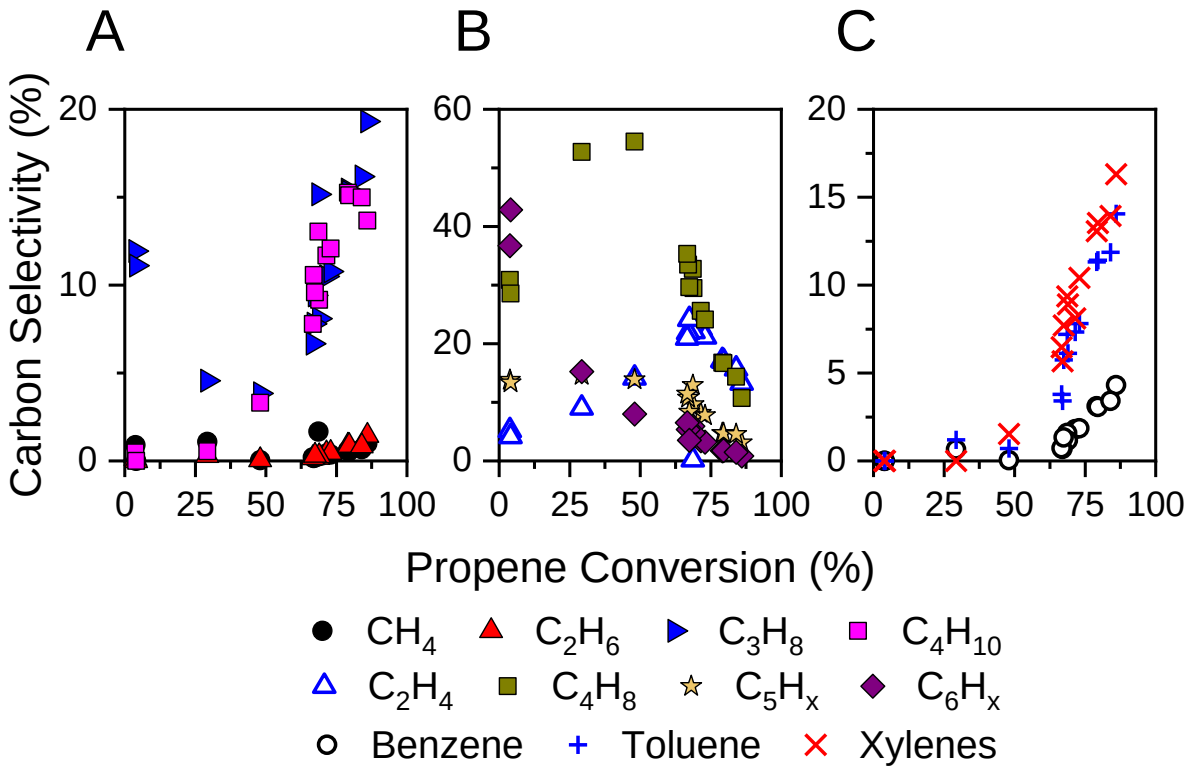

Figure 2.1. The carbon selectivity to a) light paraffins: CH_4, C_2H_6, C_3H_8, and C_4H_{10}; b) alkenes and heavy alkanes: C_2H_4, C_4H_8, C_5H_{10}, C_5H_{12}, C_5H_{12}, C_6H_{12}, and C_6H_{14}; and c) aromatics: C_6H_6, C_7H_8, and C_8H_{10} as a function of C_3H_6 conversion at 3 kPa C_3H_6 on H-ZSM-5 at 723 K.

Ethene selectivity initially increases from 4% to 27% between propene conversions of 4% to 75%, and then decreases to 13% at 86% conversion (Figure 2.1b). Similarly, initially the carbon selectivity of butene increases from 30% to 55% at propene conversions of 4% to 48%, and then decreases to 10% at 86% propene conversion. The C_5 (C_5H_{10}, C_5H_{12}) carbon selectivity decreases from 13% to 3% and C_6 (C_6H_{12}, C_6H_{14}) decreases from 43% to 0.8% with increasing propene conversions from 4% to 86%.

Selectivity towards aromatic products increases with propene conversion, from near 0% at 4% conversion to about 40% at 86% conversion (Figure 2.1c). Toluene selectivity increases from 0% to 20% and xylene selectivity increases from 0% to 16%. Benzene forms the least abundant aromatic product at 723 K; selectivity increases from 0% to 5% as propene conversion increases from 4% to 86%.

At 823 K, the methane selectivity increases from 0.2% at 1% conversion to about 10% at 97% conversion (Figure 2.2a), approximately three times higher than at 723 K. The ethane selectivity increases from 1% to 3% as the propene conversion increases from 1 to 97%. The propane selectivity rapidly decreases from 33% at 1% propene conversion to approximately 4% at propene conversions greater than about 20%. The selectivity towards butane increases slowly from undetectable levels at 1% conversion to 4% at 70% propene conversion. At higher propene conversion, the butane selectivity decreases to <0.1% at 97% conversion. The propane and butane selectivities at high propene conversion at 823 K are much lower than those at 723 K.

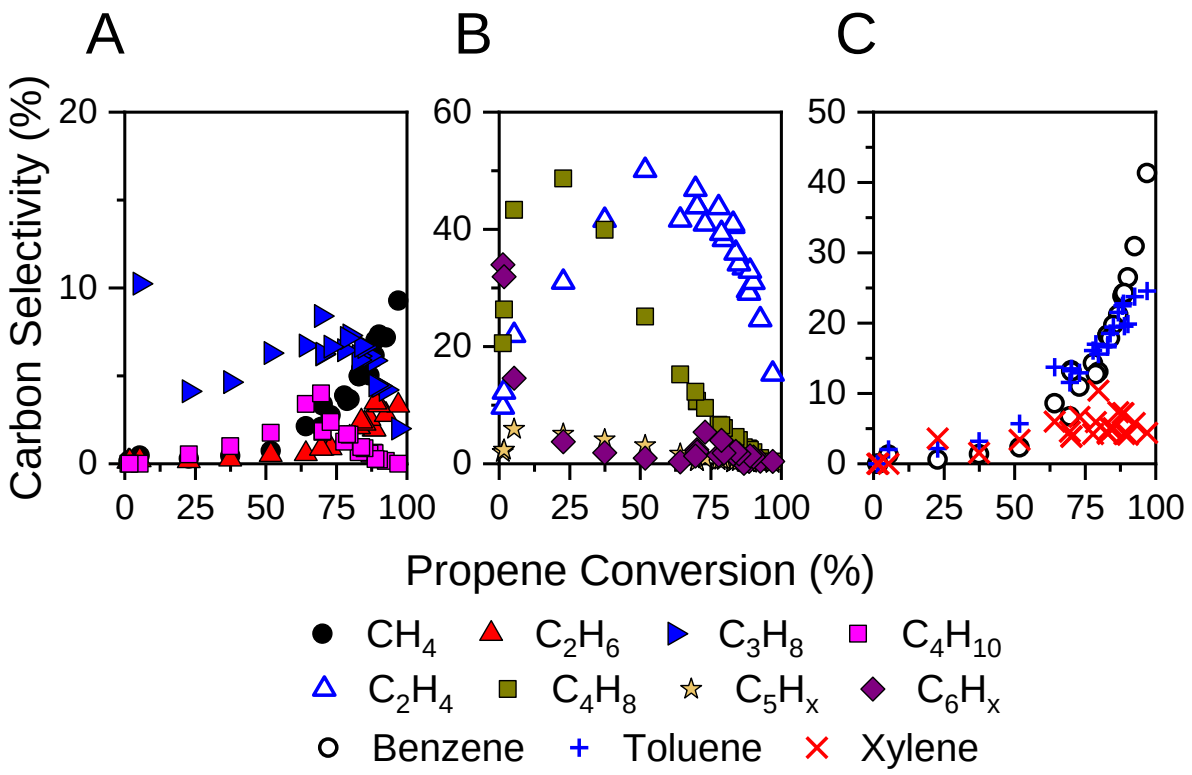

Figure 2.2. The carbon selectivity to a) light paraffins: CH_4, C_2H_6, C_3H_8, and C_4H_{10}; b) alkenes and heavy alkanes: C_2H_4, C_4H_8, C_5H_{10}, C_5H_{12}, C_5H_{12}, C_6H_{12}, and C_6H_{14}; and c) aromatics: C_6H_6, C_7H_8, and C_8H_{10} as a function of C_3H_6 conversion at 3 kPa C_3H_6 on H-ZSM-5 at 823 K.

The ethene selectivity first increases from 10% at 1% conversion to a maximum of 50% at 52% conversion, and then decreases significantly to 15% as the propene conversion increases to >90% (Figure 2.2b). The selectivity of butene at 823 K increases rapidly from 20% to 48% at propene conversions of 1% and 22%, respectively, followed by decreasing selectivity to 0.3% at 97% conversion (Figure 2.2b). The selectivity of C_5 and C_6 hydrocarbons decreases to <1% near at propene conversions above about 5%.

The selectivity to BTX aromatics increases with increasing conversion, especially above about 50% propene conversion. At near complete propene conversion, the BTX selectivity is about 70% (Figure 2.2c). Also, at 823 K, benzene is the major aromatic product with low selectivity to xylenes; while at 723 K, the xylenes are the major aromatic product with low selectivity to benzene. Two general trends are observed among the various products formed during propene aromatization. At 723 K, for one set of products, i.e., ethene, butenes, pentanes/enes, and hexanes/enes, initially

the selectivity increases with increasing conversion; while at higher conversion, these products undergo secondary reactions and the selectivity decreases to low levels as the propene conversion approaches 100%. The second set of products, i.e., methane, ethane, propane, butanes, benzene, toluene, and xylenes, increase with increasing conversion, although formation of these products generally occurs at propene conversions greater than about 50%. Methane and ethane selectivities increase with increasing conversion, although the selectivity is low. At 823 K, all products follow the same trends except for propane and butane, where the selectivity increases initially and then decreases to low levels at higher conversion. Additionally, at the higher reaction temperature, the methane selectivity significantly increases compared to that at lower temperature.

2.3.2 Product Distribution on bifunctional $PtZn/SiO_2$ + H-ZSM-5

The structure of the Pt_1Zn_1 alloy has previously been determined by in situ X-ray diffraction (XRD) and X-ray absorption spectroscopies (XAS) [29]. In this body centered, Au_1Cu_1 structure type, intermetallic alloy [30], Pt has eight Zn neighbors at 2.63 Å, and Pt is present at a non-bonding distance of 2.90 Å. This structure is highly selective for ethane [2] and propane dehydrogenation [28,29]. The catalytic performance of our catalyst was determined for propane dehydrogenation at 823 K. Similar to previous studies [29], the propylene selectivity was about 97% for propane conversions from 30 to 70% consistent with formation of the Pt_1Zn_1 intermetallic alloy.

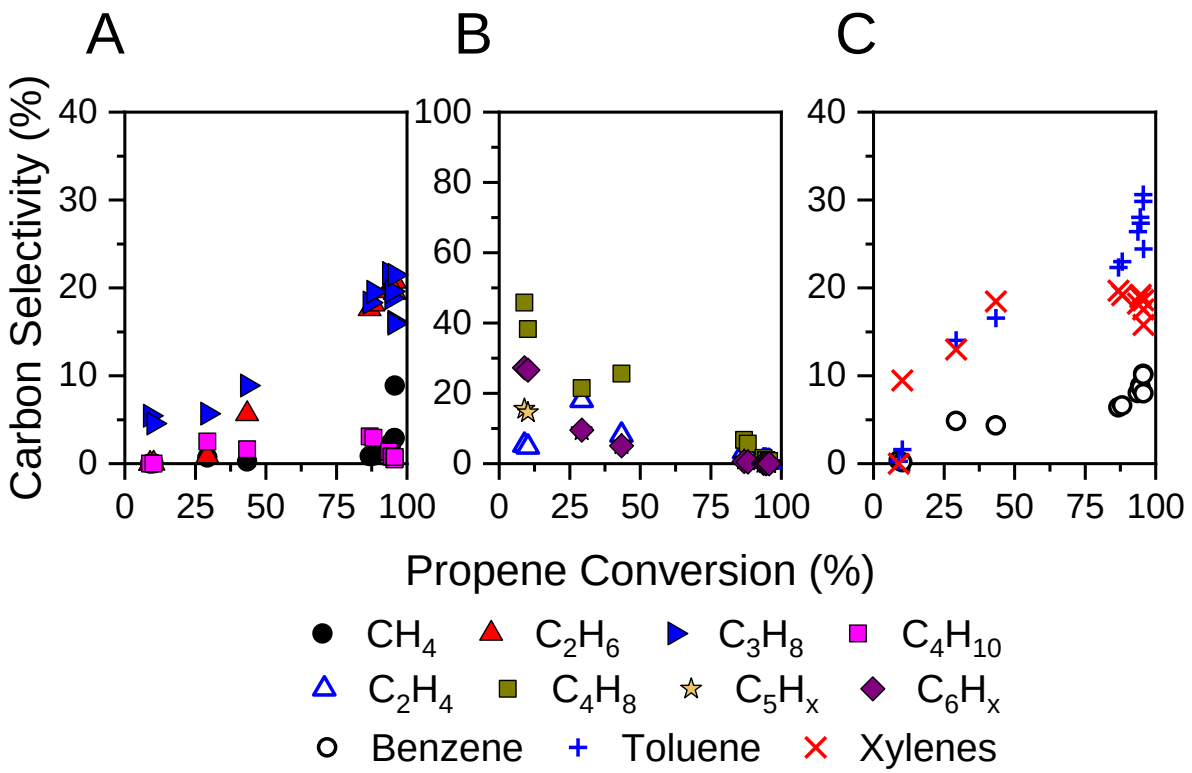

Figure 2.3. The selectivity of a) light paraffins: CH_4, C_2H_6, C_3H_8, and C_4H_{10}; b) alkenes heavy alkanes: C_2H_4, C_4H_8, C_5H_{10}, C_5H_{12}, C_5H_{12}, C_6H_{12}, and C_6H_{14}; and c) aromatics: C_6H_6, C_7H_8, and C_8H_{10} as a function of C_3H_6 conversion at 3 kPa C_3H_6 on bifunctional $PtZn/SiO_2$ + H-ZSM-5 at 723 K.

The same reaction products are formed for the bifunctional catalyst as ZSM-5 and include light alkanes: methane, ethane, propane and butane; olefins: ethylene, butenes, pentenes, and hexenes; and aromatics: benzene, toluene, and xylenes. At 723 K, the selectivity of methane and ethane is low up to about 70% propene conversion but increases to 9% and 26%, respectively, at 96% conversion (Figure 2.3a). Similar to ethane, the selectivity to propane increases from 5% to 22% across the conversion range. Unlike ethane and propane, the selectivity to butane first increases to about 7%, and then decreases to <1% at high propene conversion.

The ethene selectivity increases from 5% at 9% propene conversion to 22% at 70% conversion; while at higher conversion the selectivity decreases to <1% at 96% conversion (Figure 2.3b). Initially, the selectivities for C_4 olefins and C_5^+ hydrocarbons (C_4H_8, C_5H_{10}, C_5H_{12}, C_6H_{12}, C_6H_{14}) increase, go through a maximum, and then decrease at high propene conversion. The BTX aromatic selectivity increases with increasing conversion (Figure 2.3c). At 723 K, the selectivities

of toluene and xylenes are higher than that of benzene. All three aromatics have selectivity <2% at conversions below 50%, and then the selectivity to benzene, toluene, and xylene increase to about 5%, 15%, and 15%, respectively.

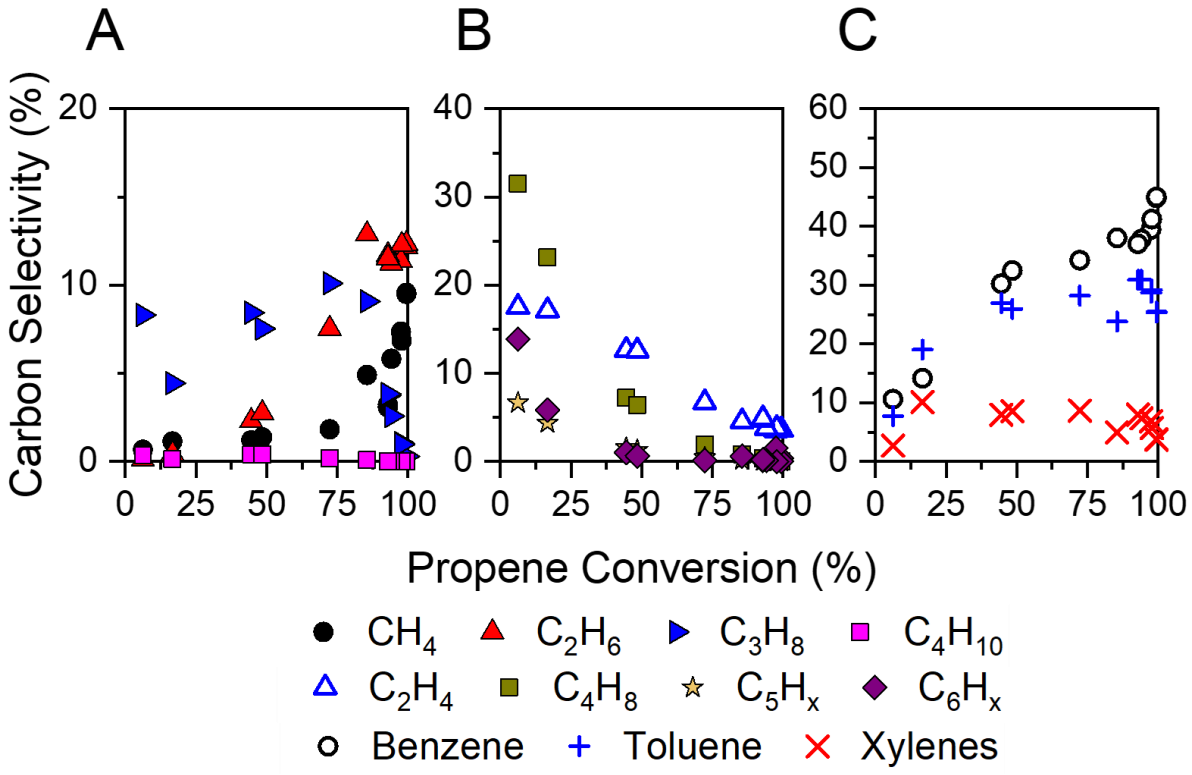

Figure 2.4. The selectivity of a) light paraffins: CH_4, C_2H_6, C_3H_8, and C_4H_{10}; b) alkenes heavy alkanes: C_2H_4, C_4H_8, C_5H_{10}, C_5H_{12}, C_5H_{12}, C_6H_{12}, and C_6H_{14}; and c) aromatics: C_6H_6, C_7H_8, and C_8H_{10} as a function of C_3H_6 conversion at 3 kPa C_3H_6 on bifunctional $PtZn/SiO_2$ + H-ZSM-5 at 823 K.

At 823 K, the methane and ethane selectivities increase from <1% at low conversion to 10% and 12%, respectively at 99% propene conversion (Figure 2.4a). The propane selectivity, however, decreases from 16% to 1% as the conversion increases. Ethene selectivity increases rapidly to 15% at 3% propene conversion, however it is lower, ca. 3%, at 99% propene conversion (Figure 2.4b). All other reactive hydrocarbons are minor products. For example, at 72% conversion, butanes and butenes comprise about 6% of products, while C_5 and C_6 hydrocarbons are less than 1%. At 823 K, the aromatics selectivity is higher than at 723 K, approximately, 80% (45% B, 30% T and 5% X) and 60% (10% B, 30% T and 20% X), respectively (Figure 2.4c).

Similar to ZSM-5, there are trends of the various products for propene aromatization with the bifunctional catalyst. At 723 K, for one set of products, i.e., ethene, butenes, butane, pentanes/enes, and hexanes/enes, initially the selectivity increases with increasing conversion; while at higher conversion, these products undergo secondary reactions and the selectivity decreases to low levels as the propene conversion approaches 100% (Figure 2.1b). The second set of products, i.e., methane, ethane, propane, benzene, toluene, and xylene, increase with increasing conversion, although high selectivities for these products, generally, occur at propene conversions greater than about 50% (Figure 2.1a and c). While methane and ethane selectivities are low at 723 K with ZSM-5, these are significantly higher for the bifunctional catalyst. Another selectivity difference is that at 723 K for ZSM-5, the butane selectivity is high, but is lower for the bifunctional catalyst and undergoes secondary reactions at higher propene conversion. At 823 K (Figure 2.2), on the bifunctional catalyst, the methane and ethane selectivities are low until about 70% conversion, but increase to about 10% for each as the at 97% propene conversion. The lower ethane and propane selectivities lead to a higher BTX selectivity at the higher reaction temperature.

2.3.3 Cyclohexene conversion on PtZn+H-ZSM-5 and H-ZSM-5

To better understand how aromatics are formed on these catalysts, a model reaction for the conversion of cyclohexene to benzene and other products was determined on H-ZSM-5 and $PtZn/SiO_2$ catalysts. ZSM-5 is highly reactive to cyclohexene (Table 1); however, the reaction products are predominantly higher molecular weight oligomeric products, with lower amounts of C_2-C_4 cracked products (Figure 2.5). Even at 94% cyclohexene conversion at 723 K, ZSM-5 forms 90% oligomeric and cracked products with approximately 10% BTX aromatics. Surprisingly, the selectivity of xylene and toluene are much higher than benzene (i.e., 0.6% benzene, 3.3% toluene, and 6.2% xylene). The rate of cyclohexene conversion on $PtZn/SiO_2$ (Table 2.1) is also high but forms primarily benzene with much smaller amounts of oligomeric products. At 94% conversion, benzene is the only aromatic product with a selectivity of 92.3%. Multiplying the conversion rates by the selectivities gives an estimate of the rate of aromatic and cracking plus oligomerization reactions. For the PtZn intermetallic alloy, the rate of aromatic formation is ten times that of ZSM-5.

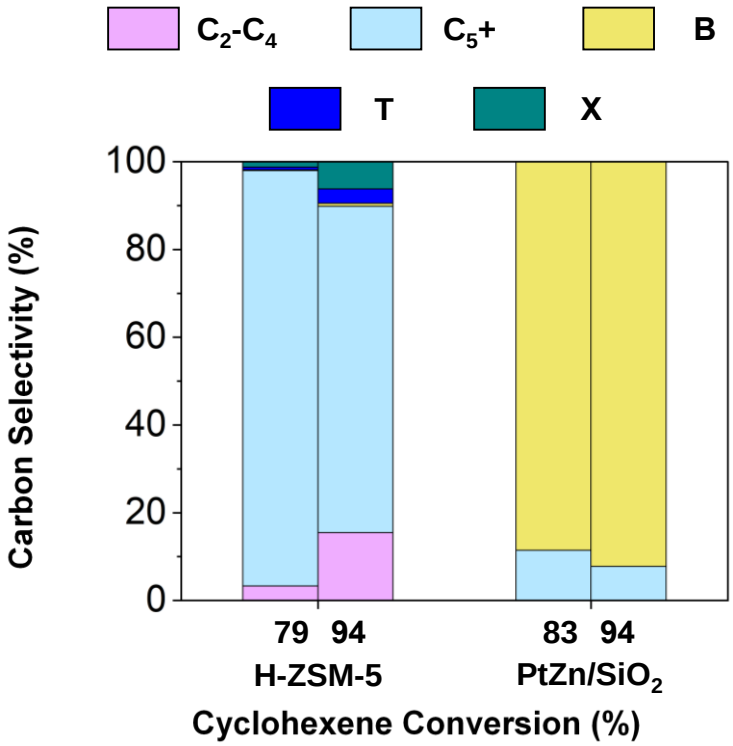

Figure 2.5. The product distribution of cyclohexene conversion on H-ZSM-5 and $PtZn/SiO_2$ at 723 K.

Table 2.1. Cyclohexene conversion, BTX formation, and cracking rates at 723 K.

Catalyst	Cyclohexene Conversion Rate 10^{-3} mol C_6H_{10} $(g_{cat}\ s)^{-1}$	BTX Formation Rate 10^{-3} mol BTX $(g_{cat}\ s)^{-1}$	Cracking Rates 10^{-3} mol $C_{2\text{-}5+}$ $(g_{cat}\ s)^{-1}$
H-ZSM-5	4.2	0.43	3.8
$PtZn/SiO_2$	4.2	3.9	0.33

2.4 Discussion

Previous studies on the conversion of olefins to aromatics concluded that bifunctional catalysts give higher BTX yields than H-ZSM-5 [11,17,18,21,31]. However, these studies compared the BTX selectivity at constant temperature and increasing space velocities or at constant space velocity and increasing temperature [17]. For example, the aromatic yields for propene conversion by ZSM-5 and bifunctional Ga oxide + ZSM-5 were determined at 773 K, 20 kPa propene, and space velocities from 0.1 – 10 g h mol^{-1}. At an equivalent space velocity of 10 g h mol^{-1}, the aromatic selectivity on ZSM-5 and Ga-ZSM-5 were 31% and 80%, respectively. Similar large differences in aromatic yields were observed at other reaction conditions; for example, at 0.1 g h mol^{-1}, the BTX selectivity on the bifunctional catalyst is 12%; while under the same conditions ZSM-5 did not produce any aromatic products. In a similar study of propene aromatization comparing ZSM-5 and bifunctional Zn-ZSM-5, the BTX selectivity at 773 K and 5.3 g mol h^{-1} was 42% for the former but 68% for the latter [18]. Similar increased aromatic yields were obtained for 1-butene conversion at 773 K and 5.3 g mol h^{-1}. The BTX selectivity was 36% on ZSM-5 and increased to 71% on Zn-ZSM-5. Each of these studies concludes that addition of a dehydrogenation catalyst to ZSM-5 increases the yields of BTX aromatics.

In each of the previous studies the aromatics selectivity is compared at constant space velocity. Thus, in Figure 2.6 the data for the bifunctional PtZn + ZSM-5 catalyst will be compared at equivalent space velocity. At both temperatures, the BTX selectivity is higher for the bifunctional catalyst at every space velocity consistent with previous studies on bifunctional Ga- and Zn-ZSM-5 catalysts. The BTX selectivity, however, is dependent on and decreases at higher space velocity. At higher space velocity the conversion is lower giving lower selectivity to aromatics. In addition, the BTX selectivity is higher at higher reaction temperature. At 723 K, the maximum BTX selectivity is about 60%; while at 823 K the BTX selectivity increases to about 80%.

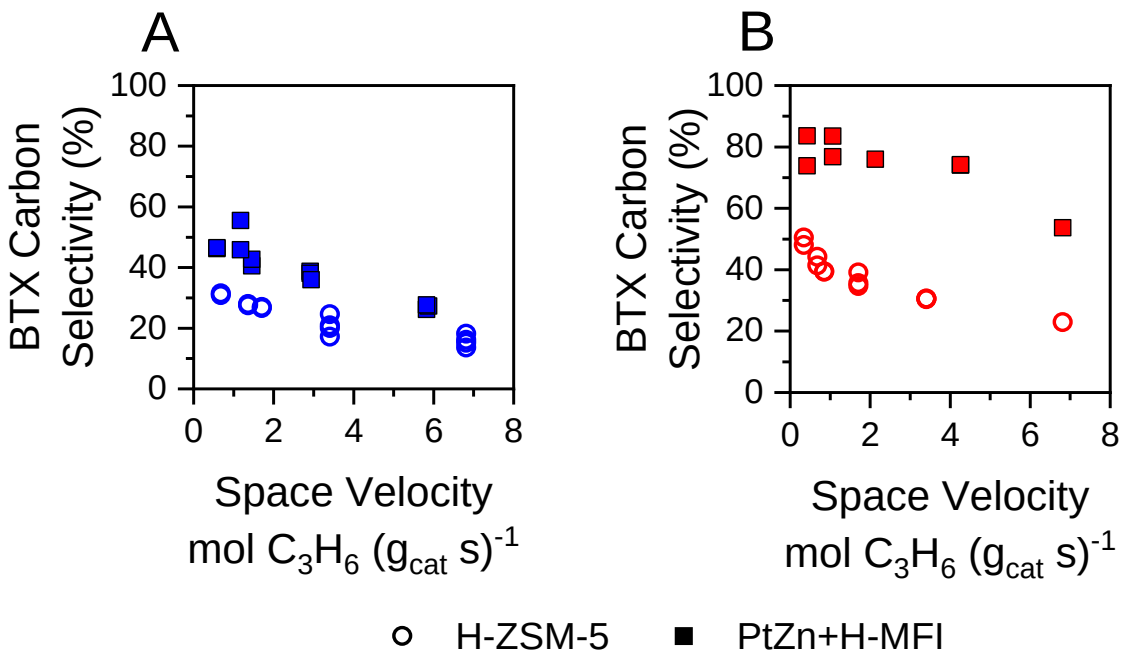

Figure 2.6. The carbon selectivity of benzene, toluene, and xylene (BTX) as a function of space velocity on H-ZSM-5 and PtZn+H-ZSM-5 at 3 kPa C_3H_6, a) 723 K (blue) and b) 823 K (red).

Since secondary reactions alter the selectivity as the conversion increases and aromatics are formed through a complex series of multiple reaction steps, to determine differences in selectivity between catalysts, one should compare at constant conversion. Figure 2.7 shows the BTX selectivities for propene conversion with ZSM-5 and bifunctional PtZn + ZSM-5 at 723 and 823 K. At both reaction temperatures, for ZSM-5 little BTX is formed until the propene conversion is greater than about 50%; while for the bifunctional catalyst, aromatics form at propene conversions of less than 10%. At propene conversion below about 90%, the BTX selectivity is always higher for the bifunctional catalyst. However, as the propene conversion approaches 100%, the BTX selectivities are very similar. Comparison of the aromatic selectivity at incomplete propene conversion would lead to the conclusion that bifunctional catalysts produce more aromatic products; while at high propene conversion, one would conclude that both catalysts give similar selectivity. Thus, the conclusion about the improved aromatics yield of bifunctional catalysts is conversion dependent.

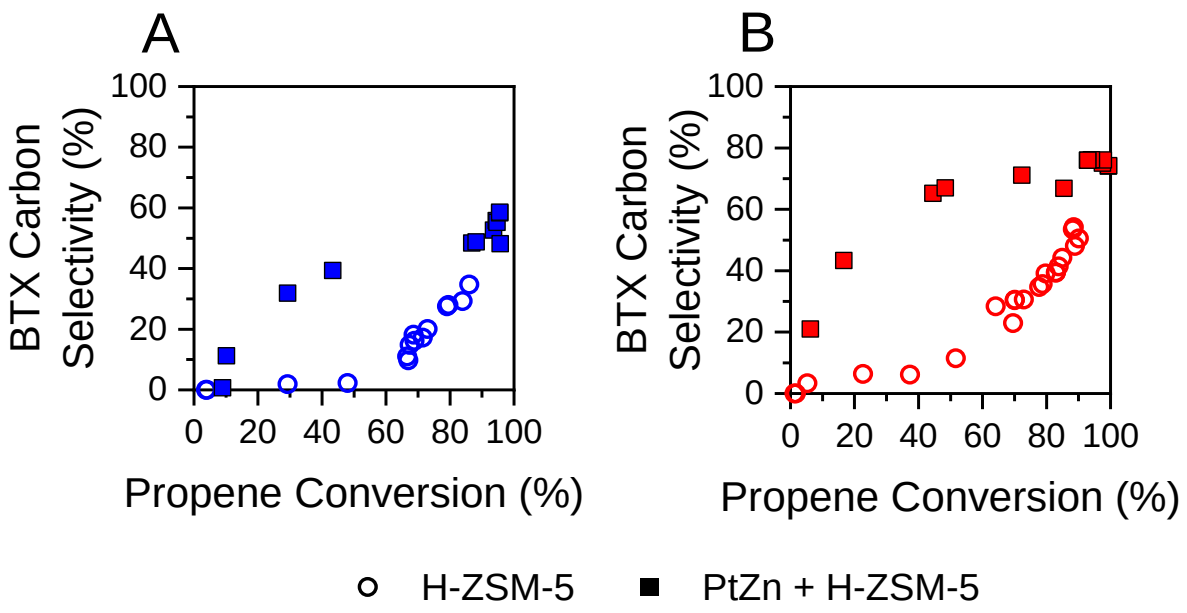

Figure 2.7. The carbon selectivity of benzene, toluene, and xylene (BTX) as a function of propene conversion on H-ZSM-5 and PtZn+H-ZSM-5 at 3 kPa C_3H_6, a) 723 K (blue) and b) 823 K (red).

Results in Figure 2.1 and Figure 2.2 indicate that there are two types of products for propene conversion, those that continually increase with increasing conversion and those where the selectivity initially increases, but at higher conversion decreases. The latter are olefins and reactive alkanes that undergo secondary reactions. For example, in Figure 2.1c, for ZSM-5 at 723 K, the butene selectivity increases to a maximum (approximately 50%) at near 50% propene conversion and then decreases to near 0% selectivity at 100% propene conversion. It is well-known that all olefins can be converted to aromatic products on ZSM-5; thus, at low propene conversions many of the initial reaction products are also reactive and will form the same products as propene. As a result, if one considers all intermediates that undergo secondary reactions to be reactants along with propene, a new conversion scale is defined.

The conversion is determined from the sum of all reactive species. As observed in Figure 2.1 and Figure 2.2, the reactive species at 723 K are ethene, butenes, C_5, and C_6 hydrocarbons (Figure 2.1b). At 823 K, in addition to ethene, butenes, C_5, and C_6 reactive intermediates, propane and butane are now reactive intermediates (see Figure 2.2b at high conversion). The conversion of propane and butane at higher temperature leads to a higher yield of aromatic products at the higher

reaction temperature. For bifunctional PtZn + ZSM-5, at 723 K, the reactive species are ethene, butenes, C_5, and C_6 hydrocarbons, equivalent to H-ZSM-5 (Figure 2.3b). However, on the bifunctional catalyst, butane is also a reactive intermediate at 723 K (Figure 2.3a), unlike ZSM-5. At 823 K, the reactive species are equivalent to those of H-ZSM-5: ethene, propane, butane, butenes, C_5, and C_6 hydrocarbons (Figure 2.4a-b).

Replotting the BTX selectivity as a function of conversion of reactive intermediates is shown in Figure 2.8. While there is some scatter at high and low conversion, using this definition of conversion, i.e., the moles of carbon reacted to non-reactive products, produces a plot where the aromatic selectivity is nearly constant over a wide conversion range. Furthermore, the selectivity of ZSM-5 and the bifunctional catalyst are very similar. For both catalysts, at 823 K, the aromatic selectivity is significantly higher than that at 723 K.

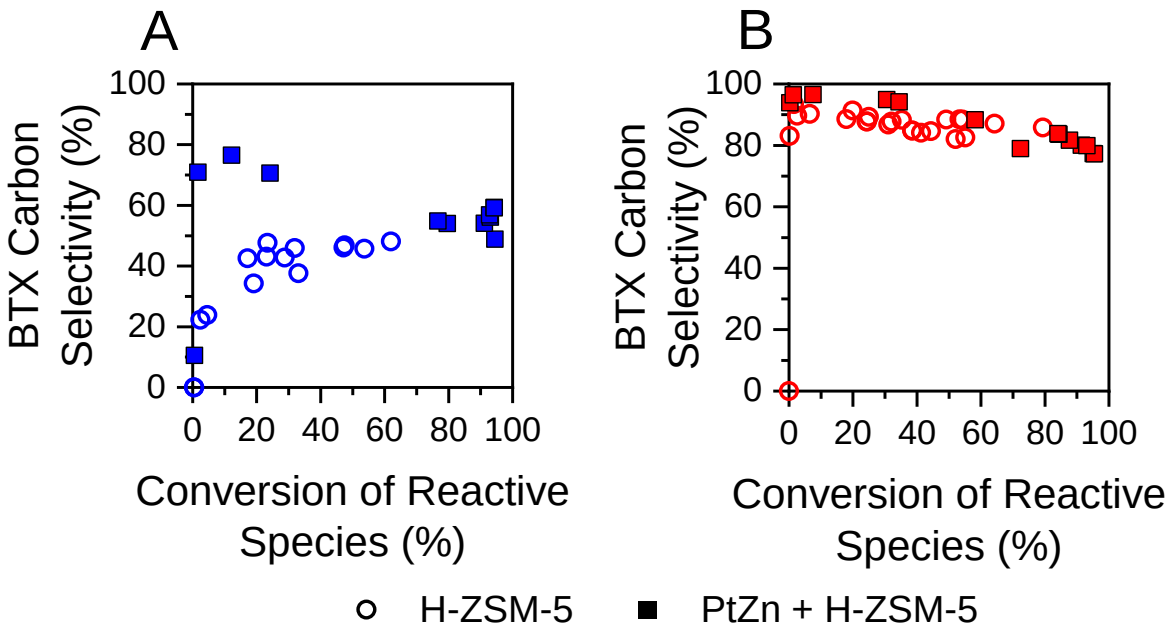

Figure 2.8. The carbon selectivity of benzene, toluene, and xylene (BTX) as a function of conversion of reactive intermediates on H-ZSM-5 and PtZn+H-ZSM-5 at 3 kPa C_3H_6, a) 723 K (blue) and b) 823 K (red).

In addition to the similar total aromatic selectivity for both catalysts (Figure 2.8), the selectivities of the individual aromatics are also very similar (Figure 2.9). This analysis shows that at 723 K, the benzene and toluene selectivities are near zero at low conversion; however, the

selectivity of both increase as the conversion increases. By contrast, the xylenes selectivity is high at low conversion, but decreases with increasing conversion. The results suggest on ZSM-5 xylenes is the primary aromatic that is formed, consistent with

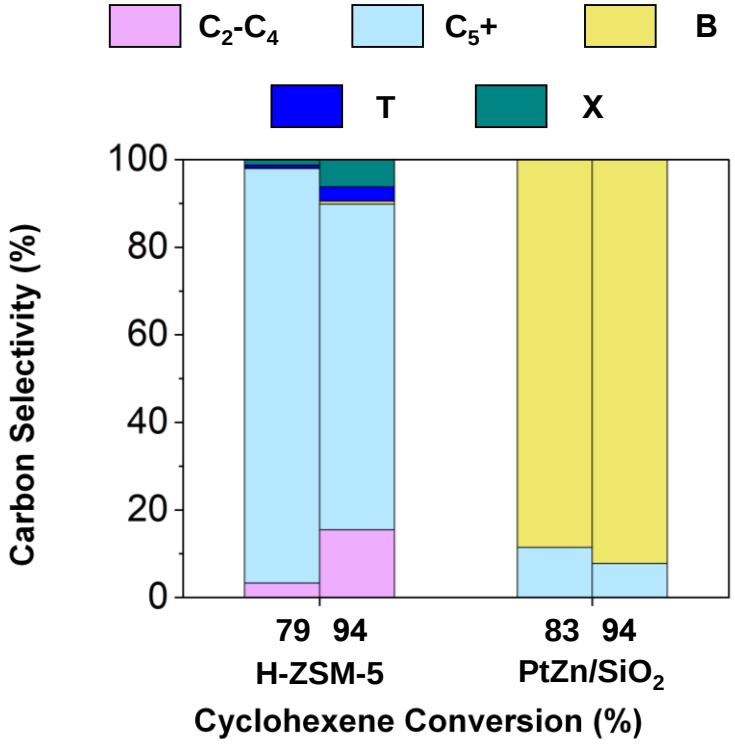

Figure 2.5 where xylenes are the dominant aromatic formed even when feeding cyclohexene as a reactant. Benzene and toluene are formed by secondary reactions at higher conversion, resulting in their lower selectivity at lower conversion. At 823 K, both toluene and xylene appear at low conversion; while benzene appears to form at higher conversion.

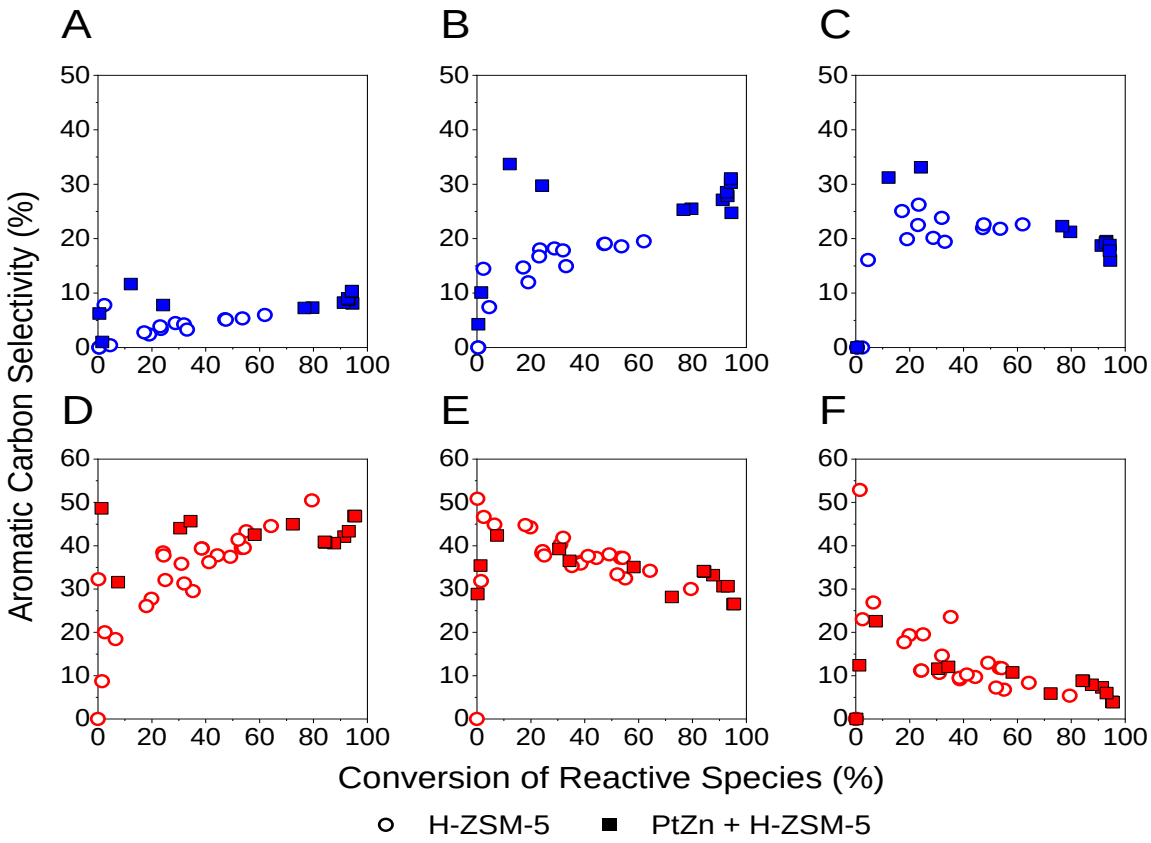

Figure 2.9. The carbon selectivity of benzene (a, d), toluene (b, e), and xylenes (c, f) at 723 K (blue: a, b, c) and 823 K (red: d, e, f) as a function of conversion of reactive intermediates.

In addition to BTX, the other final products consist of methane, ethane, propane (and butane for ZSM-5) at 723 K and methane and ethane at 823 K. At 723 K, the methane selectivities are low and similar for both ZSM-5 and the bifunctional catalyst (Figure 2.10a). At 823 K, however, there are differences depending on the catalyst (Figure 2.10b). For example, the methane selectivity at 823 K is higher on ZSM-5. This likely results from the pathways for reaction of propane and butane, which are unreactive at 723 K. However, at 823 K, monomolecular cracking of both propane and butane occurs producing methane and ethylene (from propane) and propylene (from butane). Conversion of these olefins give higher aromatic yields, but also higher selectivity to methane. For the bifunctional catalyst, at 823 K, propane and butane can form olefins and

hydrogen by dehydrogenation. Because of the high alkane dehydrogenation rate and selectivity, little methane is formed.

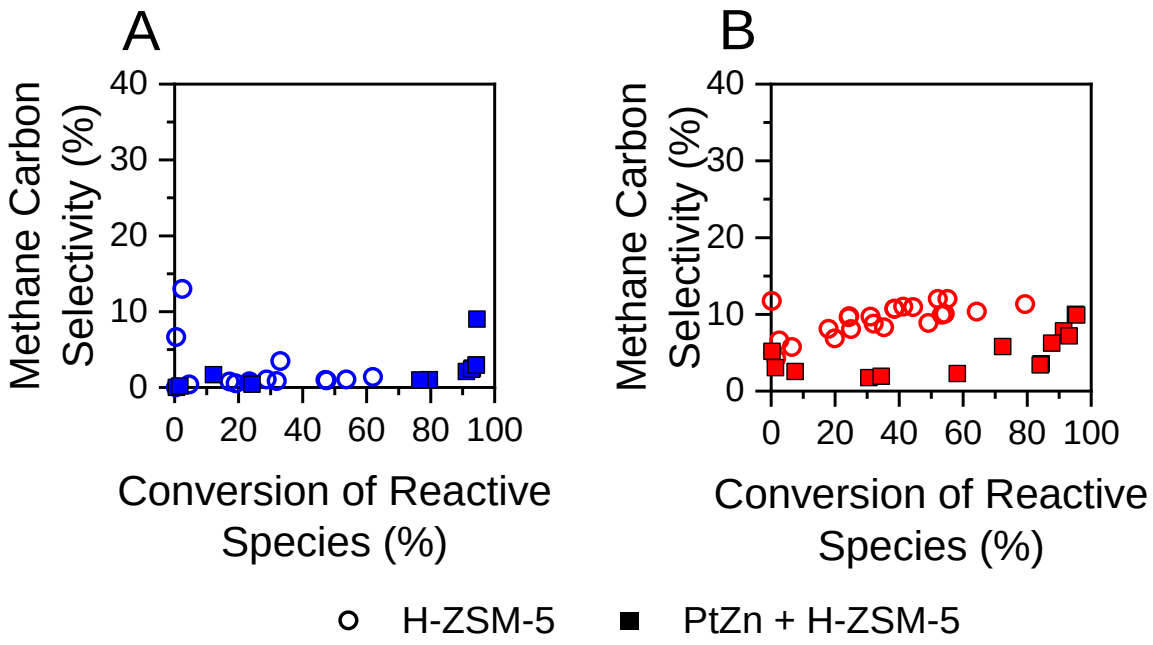

Figure 2.10. Methane carbon selectivity on H-ZSM-5 and PtZn+H-ZSM-5 as a function of conversion of reactive intermediates at a) 723 K (blue) and b) 823 K (red).

While the ethane selectivity of ZSM-5 is also low at 723 K, for the bifunctional catalyst the ethane selectivity increases significantly with increasing conversion (Figure 2.11). At 723 K, hydrogenation of ethylene is thermodynamically favored. Hydrogen, produced by naphthene dehydrogenation, saturates ethylene forming ethane. This reaction is not possible on ZSM-5. At 823 K, ethane selectivity on ZSM-5 is also low and nearly constant at all conversions. Again, on the bifunctional catalyst, ethane selectivity is higher than that of ZSM-5, but because of the higher reaction temperature the equilibrium conversion is not as high as at lower temperature, thus decreasing the selectivity.

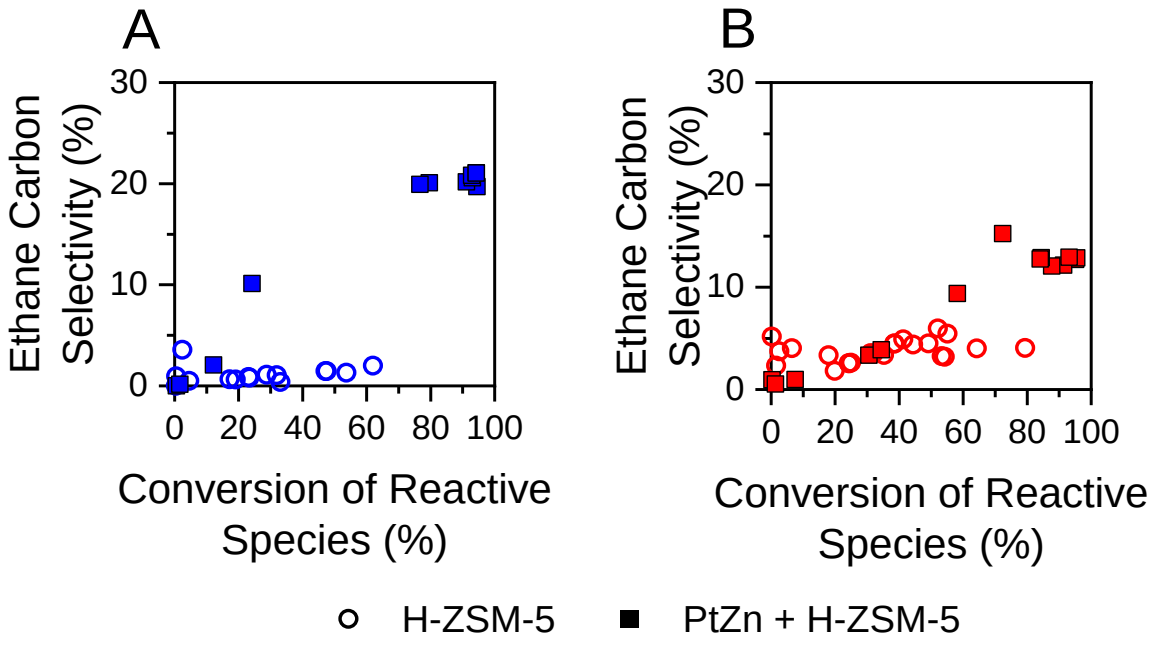

Figure 2.11. Ethane carbon selectivity on H-ZSM-5 and PtZn+H-ZSM-5 as a function of conversion of reactive intermediates at a) 723 K (blue) and b) 823 K (red).

At 723 K, propane is a non-reactive product. For ZSM-5, the propane selectivity is higher than that of the bifunctional catalyst (Figure 2.12). The aromatic formation pathway over ZSM-5 also produces 3 moles of propane [18]; while for the bifunctional catalyst, dehydrogenation leads to aromatics and H_2. These analyses indicate that for ZSM-5 there is a lower selectivity to ethane (Figure 2.11), especially at 723 K, but a higher selectivity to propane (Figure 2.12); while for the bifunctional catalyst there is a higher selectivity to ethane (Figure 2.11), but lower selectivity to propane. Additionally, butane is reactive on the bifunctional catalyst at 723 K, whereas it is not on H-ZSM-5. While the two catalysts differ in how the pathways form aromatic and non-reactive alkanes, the selectivity to total aromatic products are very similar at each reaction temperature (Figure 2.8 and Figure 2.9). When compared at constant conversion of all reactive intermediates, bifunctional catalysts do not give much higher yields of aromatics than ZSM-5 alone, although there are some differences in selectivity of the non-aromatic by-products.

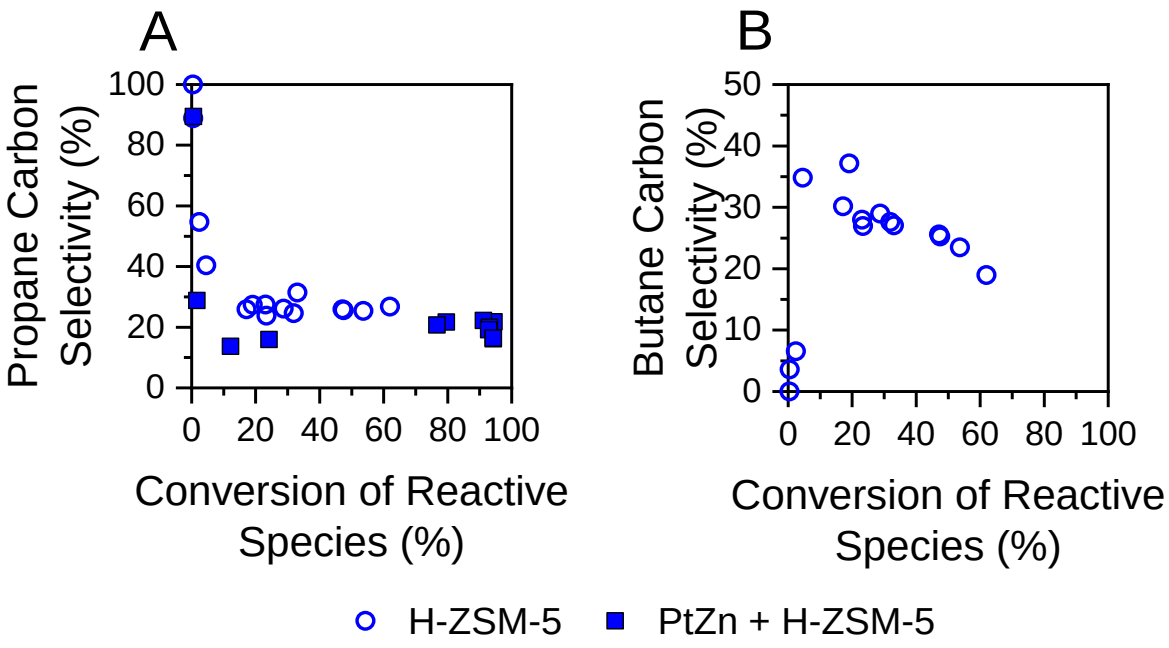

Figure 2.12. Carbon selectivity of a) propane and b) butane at 723 K on H-ZSM-5 and PtZn/H-ZSM-5 as a function of conversion of reactive intermediates.

2.5 Conclusions

This study highlights the differences between olefin conversion to BTX by ZSM-5 and bifunctional PtZn + ZSM-5 catalysts. As the reaction proceeds, there are two types of products for propene conversion, those that continually increase with increasing conversion and those where the selectivity initially increases, but at higher conversion decreases. The former are BTX and non-reactive alkanes; while the latter are olefins and reactive alkanes that undergo secondary reactions. Furthermore, the specific non-reactive alkanes differ depending on the reaction temperature. For example, propane is non-reactive at 723 K for both ZSM-5 and the bifunctional catalyst, but at 823 K is reactive on both catalysts leading to significantly higher aromatic yields at higher temperature. Conversion of all reactive intermediates at both 723 and 823 K gives very similar BTX yields for both catalysts; although because of the difference in reaction pathways, the yield of non-reactive alkanes is slightly different.

3. IMPACT OF CO-FED HYDROGEN ON HIGH CONVERSION PROPYLENE AROMATIZATION ON H-ZSM-5 AND GA/H-ZSM-5

To be submitted to Zeolite Materials and Catalysis

3.1 Introduction

Aromatics (i.e., benzene, toluene, and xylene, or BTX) are important feedstocks for the production of liquid fuels and as vital feedstocks to the modern chemical industry. Traditionally formed via the reforming of naphtha, the expanded production of shale gas has increased the desire for developing methods for converting light alkanes, especially propane and ethane, into aromatic hydrocarbons and gasoline [1]. Light alkanes may be converted to aromatics via a two-step process. In the first step, alkanes are converted to olefins and hydrogen through various processes, for example catalytic dehydrogenation or steam cracking reactions [5,6,32]. Secondly, the olefins may be converted to aromatics on zeolites or bifunctional dehydrogenation and acid catalysts [1,16–18,33–39].

Bronsted acid catalysts, in particular zeolites, have been broadly investigated for olefin conversion reactions. H-ZSM-5 has demonstrated the best performance for upgrading olefin feedstocks due to its resistance to deactivation compared to other solid acid catalysts [38]. Studies of propene aromatization generally find that H-ZSM-5 achieves aromatic selectivity around 40% for propene aromatization at 523 – 573 K. For example, Ono and co-workers report achieving 45.5% aromatic selectivity at 93.6% propylene conversion [18]. By comparison, upon the addition of Zn, aromatic selectivity has been reported to increase to 70.3% (with Zn, the conversion at equivalent space velocity is 97%). Other reports have reported similar increases in aromatic selectivity upon the introduction of Ga or Zn [16–18,33,38–40].

Additionally, previous studies explored olefin oligomerization without factoring in the effect of the hydrogen that is generated when converting alkanes to the olefin feedstock for oligomerization. Thus, these results could be achieved if hydrogen was separated between the conversion of light alkanes to olefins in the process mentioned above. However, this separation is prohibitively expensive, thus it is necessary to understand how the presence of equimolar H_2 affects the product distribution of olefin aromatization. In particular, the presence of equimolar H_2

would be expected to suppress the enhanced performance of the dehydrogenation functionality on these catalysts if the increases in aromatic formation are due to enablement of dehydrogenation pathways for aromatic generation.

Herein, the product distribution of propylene aromatization on Ga-impregnated H-ZSM-5 is compared to that on H-ZSM-5 in the presence and absence of equimolar co-fed H_2 and at 1.9 kPa and 50 kPa. Comparisons of the product distribution on both catalysts suggest that Ga enhances aromatic selectivity by enabling production of aromatic rings via catalytic dehydrogenation. The effect of increasing the partial pressure of C_3H_6 and H_2 shifts the olefin hydrogenation equilibrium to favor paraffin production, thereby reducing the differences observed between Ga/H-ZSM-5 and H-ZSM-5. The effect of equimolar H_2 is demonstrated to have minimal impact on the product distribution of H-ZSM-5, although on Ga/H-ZSM-5 it shifts the product distribution to favor oligomerization products over the formation of aromatics at high conversions in the presence of high partial pressures of propylene and hydrogen.

3.2 Methods

3.2.1 Catalyst Synthesis

To produce a 10 g batch of catalyst, 10 g commercial ammonium form ZSM-5 extrudate (SiO2/Al2O3 = 30, H-ZSM-5/Al_2O_3 = 4, Zeolyst International, CBV 3014) was calcined at 550 °C for 3 hrs (5 °C/min ramp rate) to convert the catalyst to H^+-form ZSM-5 (H-ZSM-5). Ga/H-ZSM-5 was then produced by adding Ga to the H-ZSM-5 via incipient wetness impregnation, targeting 3 wt.% Ga (g Ga/g extrudate, including Al_2O_3). A Ga^{3+} solution was prepared by dissolving 1.1 g gallium nitrate hydrate (Sigma Aldrich) and 0.83 g citric acid (Sigma Aldrich) in 5 mL Millipore water to achieve a 1:1 mol ratio of Ga:citrate. This solution is then added dropwise to the H-ZSM-5 extrudate while mixing mechanically using a plastic spatula. The solution was then dried overnight at room temperature and calcined at 550 °C for 3 hrs (5 °C/min ramp rate).

3.2.2 Catalyst Performance Testing

Catalytic performance was evaluated by loading catalyst in a quartz tube fixed bed reactor (10.5 mm i.d.) equipped with mass flow rate controllers (Parker Porter, CM400) for atmospheric pressure conditions. A furnace (Applied Test Systems series 3210) was connected to a temperature

controller to supply the heat and maintain the desired temperature. Reactions were performed at two different partial pressures of propylene and hydrogen: 1.9 kPa and 50 kPa. During a reaction at 1.9 kPa, 3% C_3H_6 (balance N_2, Indiana Oxygen) and 5% H_2 (Indiana Oxygen) were diluted in ultrahigh purity N_2 (99.99%, Indiana Oxygen) and co-fed to achieve equimolar 1.9 kPa C_3H_6 and H_2 or 1.9 kPa C_3H_6 at equivalent space velocities in different trials. At 50 kPa, the reactor is co-fed with pure propylene (≥99.98%, Indiana Oxygen) and pure H_2 (Indiana Oxygen). For comparison, equivalent reactions were performed by replacing the H_2 with N_2 to affect equivalent partial pressures of C_3H_6 at equivalent space velocities.

Catalysts were supported on quartz wool with a K-type thermocouple placed in the middle of the bottom of the catalyst bed to monitor the temperature in the bed. Reactor effluent was discharged through a line heated to 170 °C using heat tape (Omega) and fed to a gas chromatograph (Agilent 6890A) equipped with a flame ionization detector (Agilent J&W HP-1 column, 0.320 mm i.d. × 25m) for reactant and product quantification. The catalytic performances were evaluated at 450 °C and atmospheric pressure. The conversion and product selectivity were obtained at different space velocities corresponding to 25 - 160 ccm (STP) in combined flowrate.

Product selectivities and reaction conversion were determined based on the relative peak area as measured from gas chromatography assuming conservation of carbon throughout the reaction. Thus, selectivities are mildly overestimated as large carbonaceous species trapped in the catalyst bed (i.e., coke) and those that liquefy in the lines are not accounted for. No liquid buildup in the lines is observed for experiments conducted while feeding 2.9 kPa C_3H_6. At 50 kPa C_3H_6, small amounts of liquid deposition on the walls of the reactor tube at the exit of the clamshell furnace are observed.

3.2.3 X-ray Absorption Spectroscopy

X-ray absorption spectroscopy (XAS) measurements were taken at the 8-ID beamline of the National Synchrotron Light Source II at Brookhaven National Lab. Measurements were taken at the Ga K-edge (10,367 eV) in fluorescence mode. Samples were ground into a powder, pressed into a wafer, and sealed using Kapton tape, and then placed on the beamline for scanning. Scans were taken from 10,167 – 11,350 eV.

To process data, WinXAS 3.1 software was employed using standard procedures for fitting. Normalization of the absorption spectra was performed by fitting a 1st degree polynomial to the

pre-edge region (10,167 – 10,315 eV) and a 3rd degree polynomial to the absorption region above the edge (10,412 eV – 11,350 eV). The absorption spectrum was then converted to photon momentum space (k-space) and a cubic spline fit with 5 splines was fit to the absorption spectrum corresponding to the 2 – 12 k, and the resultant $\chi(k)$ spectrum was weighted by a factor of k^2. The Fourier transform of the $\chi(k)*k^2$ spectrum from k = 2.5 – 10.5 was then utilized to generate the phase-unshifted r-space spectrum, which was fit with experimental Ga-O scattering path. The phase shift and amplitude of the experimental Ga-O scattering path was determined by isolating the first shell of the r-space spectrum of a gallium (III) acetylacetonate, $Ga(AcAc)_3$, standard (Sigma Aldrich) with 6 Ga – O bonds at 1.94 Å. The phase shift and amplitude of this experimental scattering path was then used in combination with the EXAFS equation to perform a least-squares fit of the coordination number and bond distance of the Ga/H-ZSM-5 sample.

3.2.4 Elemental Analysis

Energy dispersive X-ray fluorescence (EDXRF) data were collected using a Malvern Panalytical Epsilon4 X-ray fluorescence spectrometer equipped with a 15 W silver anode X-ray tube, a ten-sample changer, and helium gas flush option, and an energy dispersive silicon drift detector. Samples were packed as powders into polypropylene XRF cups of appropriate sizes. Prior to data collection, a recalibration standard based on elements Al, Ca, Fe, K, Mg, Na, P, S and Si was measured for drift correction in the soft X-ray region. Data were collected using the Epsilon software employing the "Omnian" data collection procedure [41]. Data were collected with six different acceleration voltages between 5 and 50 kV and varying thickness Ti, Al, Cu and Ag filters. Data were analyzed using the standardless Omnian procedure, with data processing parameters being defined prior to analysis for each type of sample using the Epsilon Dashboard software [42].

3.3 Results

A large number of products are observed (i.e., isomers of alkanes and alkenes containing $C_4 – C_{7+}$); thus, products with four or more carbons have been grouped by carbon number, with the exception of benzene, toluene, and xylene. Additionally, products are discussed in the following order: aromatics (i.e., benzene, toluene, and xylene); light alkanes (i.e., methane, ethane, and propane), and reactive intermediates (i.e., ethylene, C_4, C_5, C_6, and C_{7+} species).

3.3.1 Product Distribution on H-ZSM-5 with and without H_2

The conversion of propylene and other olefins to aromatics and hydrocarbons has been extensively studied. Here, we compare the products of propylene conversion with and without equimolar amounts of co-fed H_2 at 723 K by comparing the product distribution of C_3H_6 aromatization at 50 kPa and 1.9 kPa partial pressure (balance N_2). The space velocity was varied to give propylene conversions from about 30% to above 95%. The aromatic distribution (Figure 3.1) while feeding 50 kPa C_3H_6 are similar when cofeeding 50 kPa H_2 or N_2. All three aromatics (i.e., benzene, toluene, and xylene) have selectivities <2% up to conversions about 70% (Figure 3.1, squares). At propylene conversions above 70%, selectivity to benzene (Figure 3.1a), toluene (Figure 3.1b), and xylene (Figure 3.1c) increase substantially, ultimately reaching selectivities within error of 7%, 15%, and 9%, respectively.

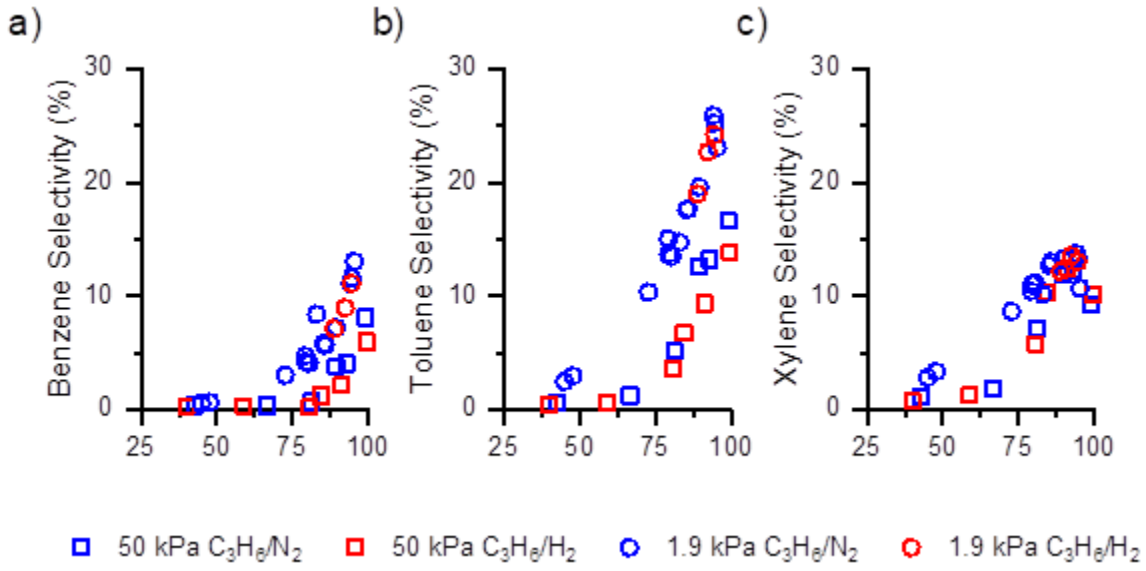

Figure 3.1. The carbon selectivity to a) benzene, b) toluene, and c) xylenes as a function of propylene conversion in the presence and absence of 1.9 kPa H_2 on H-ZSM-5 at 723 K, 1.9 kPa C_3H_6, balance N_2.

Methane and ethane selectivities (Figure 3.2a and b, respectively) are <5% at all conversions, increasing from selectivities <0.1% until conversions around 80%, at which point they increase to approximately 2%. The low selectivity to methane indicates that monomolecular cracking does not contribute significantly to the reaction mechanism until high conversions, if at

all. This is consistent with high concentrations of olefins inhibiting monomolecular cracking, as reported by Krannila et al. [6]. The selectivity to propane (Figure 3.2c), however, follows a significantly different trend. Propane selectivity increases from 5% at 45% conversion to 24% at 95% conversion, making it one of the largest by-products of propylene aromatization. The similar selectivity with and without co-fed H_2 is consistent with previous reports that Bronsted acid (H^+) catalysts are not active for hydrogenation or dehydrogenation reactions. This suggests propane is formed via cracking mechanisms, which has been reported as a product of cracking of higher molecular weight hydrocarbons [32].

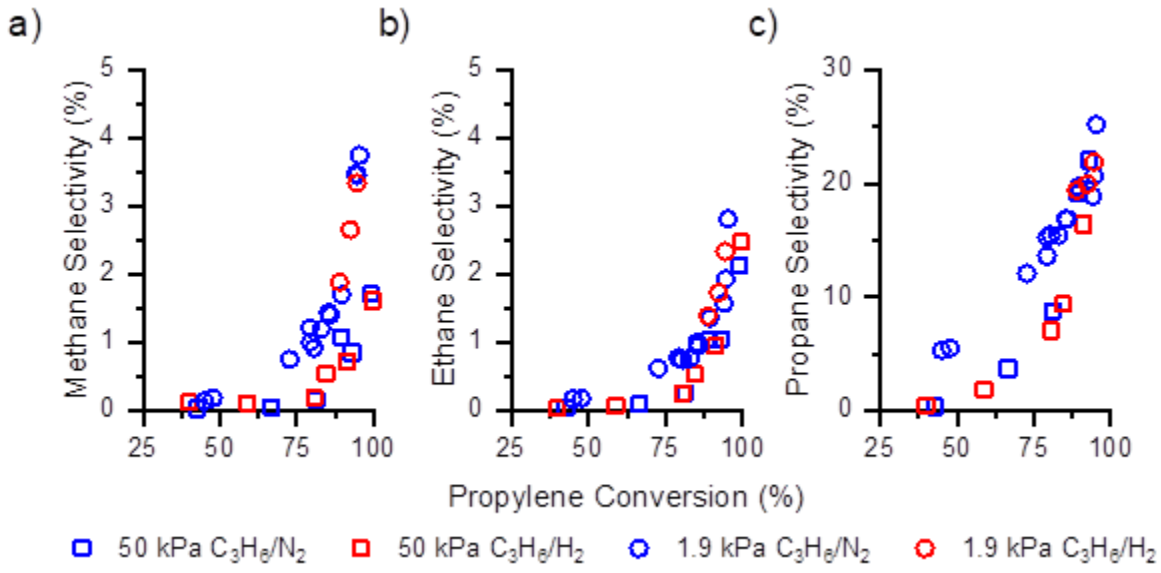

Figure 3.2. The carbon selectivity to a) methane, b) ethane, and c) propane as a function of propylene conversion in the presence and absence of 1.9 kPa H_2 on H-ZSM-5 at 723 K, 1.9 kPa C_3H_6, balance N_2.

In addition to aromatics and light alkanes, the remaining products are ethylene and higher molecular weight hydrocarbons (i.e., with 4 or more carbons). Whereas aromatic and light alkane selectivities monotonically increased (Figure 3.1 and Figure 3.2), the selectivity to these products initially increase, and then decrease as conversion continues to increase (Figure 3.3). At 50 kPa, ethylene selectivity increases to 6% at 80% conversion, and then decreases to <1% selectivity at conversions >95% (Figure 3.3a). C_4 (Figure 3.3b), C_5 (Figure 3.3c), C_6 (Figure 3.3d), and C_{7+} (Figure 3.3e) all have maximum selectivities at conversions lower than the lowest conversion tested in this study (40%) and ultimately reach 13%, 3%, <1%, and approximately 15%, respectively. At high

conversions, the presence of condensed liquids at the outlet of the reactor were observed, suggesting small amounts of high molecular weight products are formed. This may be the reason that significantly more scatter is present in the C_{7+} selectivity observed at high conversions.

At a lower partial pressure of 1.9 kPa C_3H_6, the selectivity to each aromatic is <5% until 50% propylene conversion (Figure 3.1, circles). Benzene selectivity increases from <1% at 45% conversion to 13% at 95% conversion. Toluene is the most abundant aromatic formed, increasing from 3% to 25% across the same range tested. Xylene selectivity at conversions <75% are similar to that of toluene, increasing from 3% to 9% as conversion increases from 45% to 73%, however as conversion continues to increase, the selectivity to xylene only increases to 13% at 95% conversion. The aromatic distribution is equivalent when co-fed H_2. Methane (Figure 3.2a) and ethane (Figure 3.2b) selectivity at 1.9 kPa are <5% across all conversions, increasing from <1% at propylene conversions below 70%. As conversion increases beyond 70%, methane and ethane selectivity increase to about 3%. Ethylene, C_4s, C_5s, C_6s, and C_{7+} species selectivity increases to a maximum value at intermediate conversions, and then decreases at higher conversions due to secondary reactions. The maximum selectivity to ethylene (Figure 3.3a) occurs somewhere between 48% and 73% conversion, while the maxima for the other reactive intermediates occurs at conversions ≤ 45% (the lowest conversion tested).

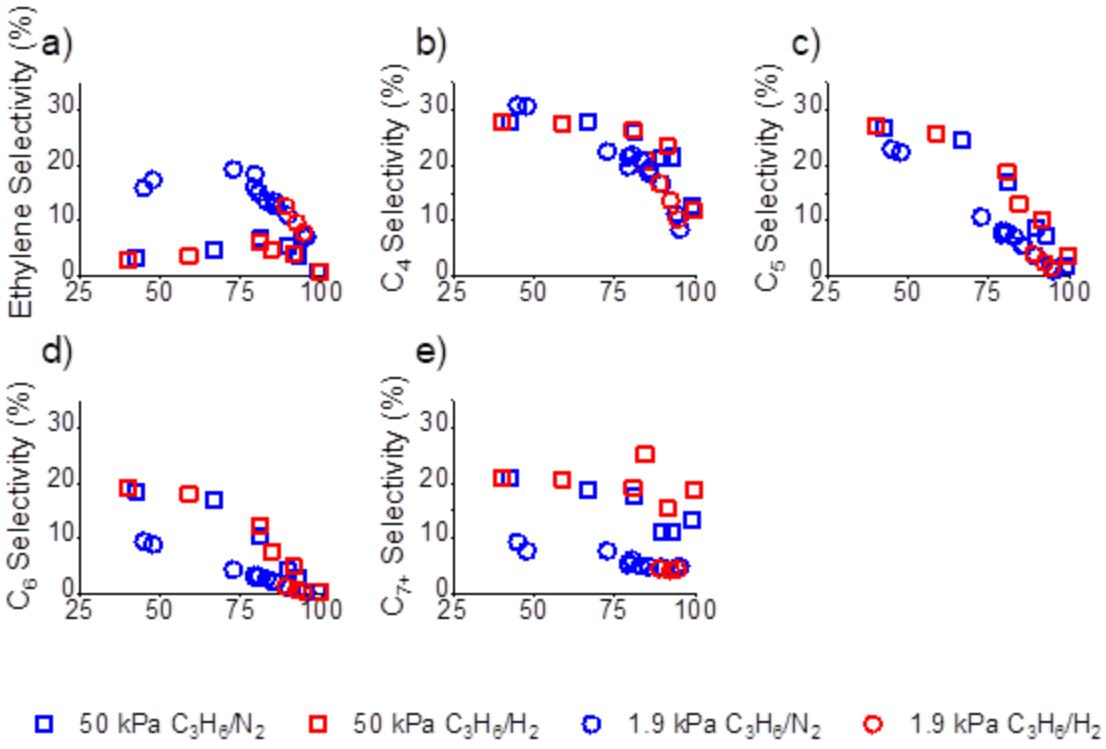

Figure 3.3. The carbon selectivity to reactive intermediates: a) ethene, b) butanes/enes (C_4), c) pentanes/enes (C_5), d) hexanes/enes (C_6), and e) larger non-aromatic hydrocarbons, C_{7+} as a function of propylene conversion in the presence (red) and absence (blue) of equimolar H_2 on H-ZSM-5 at 723 K at 1.9 kPa C_3H_6/N_2 (circles) or 50 kPa C_3H_6 (squares).

3.3.2 Catalyst Characterization

To determine the coordination geometry and bond distance between the Ga and neighboring atoms, X-ray absorption spectroscopy (XAS) was performed at the Ga-K edge. XAS can be decomposed into two regions: X-ray Absorption Near Edge Spectroscopy (XANES) and Extended X-ray Absorption Fine Structure (EXAFS). XANES provides information regarding the coordination geometry and oxidation state of the Ga, while numerical fitting of the EXAFS region yields the number of bonds and bond distance between Ga and surrounding atoms. Herein, the XANES of Ga/H-ZSM-5 is compared to gallium acetylacetonate, $Ga(AcAc)_3$; (Figure 3.4a). $Ga(AcAc)_3$ has octahedrally (Oh) coordinated Ga^{3+} ions surrounded by six Ga-O bonds with bond distance of 1.94 Å.

The XANES of Ga/H-ZSM-5 has an edge energy, defined as the inflection point in the initial rise in absorption, of 10,372.6 eV, and a white line energy (i.e., the energy at which the first

maximum absorption occurs) of 10,376.2 eV (Figure 3.4a). Beyond the white line, there are shoulders near 10,381 eV, which has been previously reported to be characteristic of tetrahedral Ga^{3+} [43–46]. By comparison, the edge energy and white line energy for $Ga(AcAc)_3$ is 10,376.5 and 10,379.0 eV, respectively.

Table 3.1. Characteristic XANES energies (10,350 – 10,400 eV)

Sample	Edge Energy eV	White Line Energy eV	Coordination Geometry
Ga/H-ZSM-5	10,372.6	10,376.2	Td
$Ga(AcAc)_3$	10,376.5	10,379.0	Oh

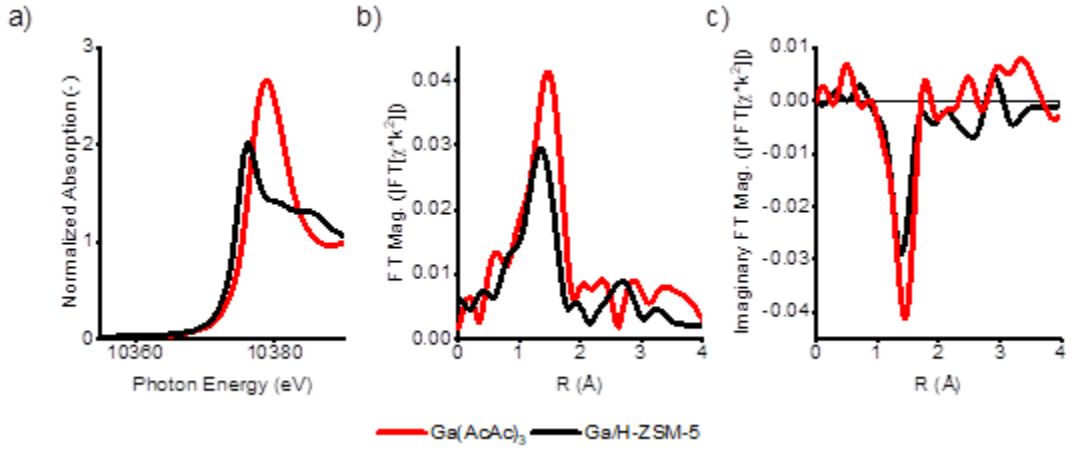

Figure 3.4. The a) XANES region (10,350 – 10,400 eV) and the b) real and c) imaginary portions of the Fourier transform of the EXAFS regions for $Ga(AcAc)_3$ and Ga/H-ZSM-5. Materials were scanned ex-situ in He at ambient temperature.

The white line energy for $Ga(AcAc)_3$ (10,379.4) is consistent with octahedral Ga^{3+}. Ga/H-ZSM-5 does not have a prominent absorption feature at 10,379 eV, indicating that octahedral Ga^{3+} is not present. Similarly, Ga/H-ZSM-5 has a lower XANES energy when compared with $Ga(AcAc)_3$, suggesting that the Ga present in Ga/H-ZSM-5 is tetrahedral Ga^{3+}.

Qualitative comparison of the Fourier transform of the EXAFS region of $Ga(AcAc)_3$ and Ga/H-ZSM-5 and quantitative fitting of the EXAFS region of Ga/H-ZSM-5 are consistent with the formation of tetrahedral Ga^{3+} in Ga/H-ZSM-5. The Ga/H-ZSM-5 first shell is the prominent feature near R = 1.35 Å (Figure 3.4b, phase uncorrected distance). By comparison, $Ga(AcAc)_3$ has a first

shell peak at 1.45 Å, consistent with having a longer bond distance. The intensity of the first shell is significantly higher for $Ga(AcAc)_3$ compared to Ga/H-ZSM-5, indicating that Ga/H-ZSM-5 has fewer Ga-O bonds than $Ga(AcAc)_3$. This is supported by numerical fitting of the EXAFS (Table 3.1), where results confirm the formation of 4.0 Ga-O bonds at 1.84 Å, consistent with previous results indicating the formation of Ga^{3+} single sites [47]. Tetrahedral Ga^{3+} with an average bond distance of 1.84 Å has been previously reported as the active form of Ga for propane dehydrogenation and aromatization on Ga/H-MFI [43,48] and on Ga/SiO_2 [47].

Table 3.2. EXAFS Numerical Fitting Parameters

Sample	CN (±10%)	R (± 0.02 Å)	σ^2	E_0
$Ga(AcAc)_3$ ref.*	6*	1.94*	0.005	-1.54
Ga/H-ZSM-5	4.0	1.84	0.005*	-1.67

**Values held fixed*

3.3.3 Product Distribution on Ga/H-ZSM-5 with and without H_2

Ga/H-ZSM-5 is the most widely studied bifunctional catalyst for dehydroaromatization due to its demonstrated higher selectivity to aromatics than H-ZSM-5 [17,18,34,36,38,39]. For this reason, Ga/H-ZSM-5 was also studied for olefin aromatization in the presence and absence of equimolar H_2. Previous literature has studied olefin aromatization on Ga/H-ZSM-5 [17,33–35,37,39,47,49]. However, since Ga is a known dehydrogenation catalyst [5,43,50], the principal of microscopic reversibility suggests that it is also reactive for olefin hydrogenation, which may affect the product distribution of olefin aromatization by hydrogenating olefins to form paraffins. Here, the product distribution of C_3H_6 aromatization was determined across a range of conversions achieved by changing the space velocity at 723 K and 1.9 kPa C_3H_6 or 50 kPa C_3H_6 in the presence or absence of equimolar H_2.

Whereas on H-ZSM-5 feeding either H_2 or N_2 resulted in no significant differences any products, trends on Ga/H-ZSM-5 differ between co-fed H_2 and N_2 at 50 kPa. Toluene selectivity (Figure 3.5b) is similar at conversions below 70% in the presence of H_2 or N_2, with a selectivity <2%. However, at conversions above 70%, where toluene selectivity becomes more appreciable, the selectivity in N_2 increases more rapidly, reaching a selectivity of 20% at 95% conversion compared to only 14% when co-feeding H_2. Xylene follows a similar trend (Figure 3.5c), where

xylene selectivity is ≤3% at conversions below 72%, and then increases more rapidly in N_2 than H_2, reaching selectivities of 22% and 14%, respectively. Benzene is produced in smaller amounts at 50 kPa, reaching 5% and 3% selectivity at 95% conversion in N_2 and H_2, respectively (Figure 3.5a).

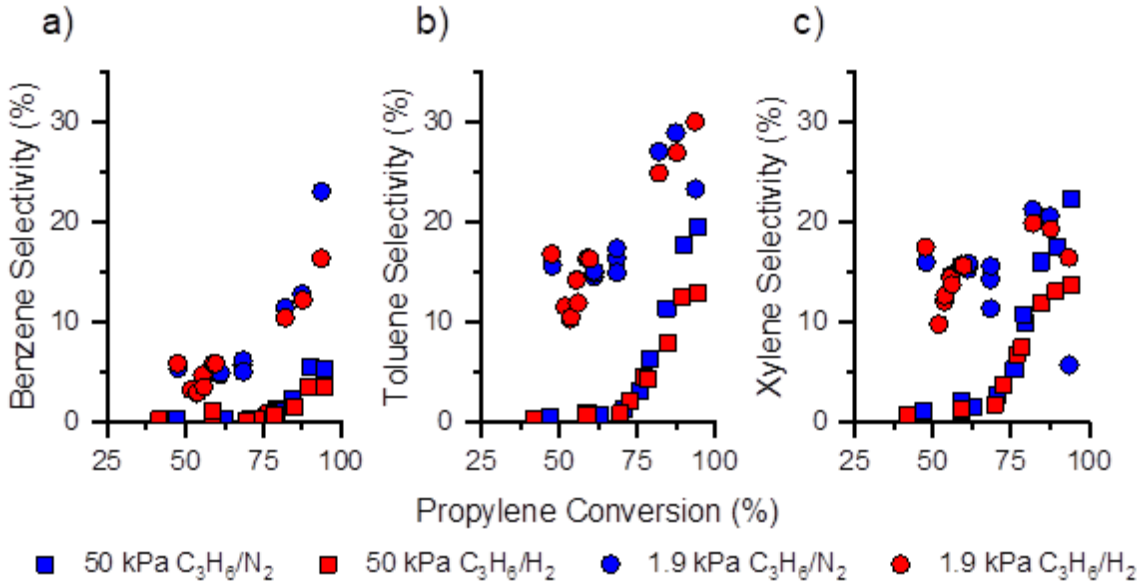

Figure 3.5. The carbon selectivity to a) benzene, b) toluene, and c) xylene as a function of propylene conversion in the presence and absence of 1.9 kPa H_2 on Ga/H-ZSM-5 at 723 K, 1.9 kPa C_3H_6, balance N_2.

At 50 kPa C_3H_6 (Figure 3.6, squares) methane and ethane selectivity both remain <0.3% up to 80% conversion, and then increases to 1.4% and 1.2% selectivity at 95% conversion, respectively. Propane selectivity slowly increases from 0.3% selectivity at 47% conversion to 5% at 80% conversion before more quickly increasing to 10% selectivity at 95% conversion. C_2H_4, C_4, C_5, C_6, and C_{7+} selectivities decrease as conversion approaches complete conversion (Figure 3.7). Additionally, with the exception of C_4 selectivity at 50 kPa, the selectivity to reactive intermediates is unaffected by the co-feed of H_2. The ethylene selectivity is lower, remaining constant (≈ 3%) from 47% to 62% conversion, then increasing to 8% selectivity at 80% conversion, and then decreasing to 3% at 95% conversion. At 50 kPa (squares), the selectivity trends for C_4 are different when co-feeding H_2 (red) compared to co-feeding N_2 (blue). In N_2, C_4 selectivity is relatively constant (≈27%) from 47 – 75% conversion, and then decreases to 16% selectivity at

95% conversion. In H_2, C_4 selectivity remains approximately 27% across the entire conversion range. This 10% difference only occurs at very high conversions (≥85%), and is predominantly offset by differences in aromatic selectivity of 3% to each of the aromatics (Figure 3.5). At 50 kPa, C_5 and C_6 selectivity are approximately constant 47 – 70% conversion (at 27% and 18%, respectively), and then decreases to 5% and 2%, respectively, as conversion increases to 95%. At 50 kPa (squares), the C_{7+} selectivity decreases from 21% to 13% as conversion increases from 47% to 95%.

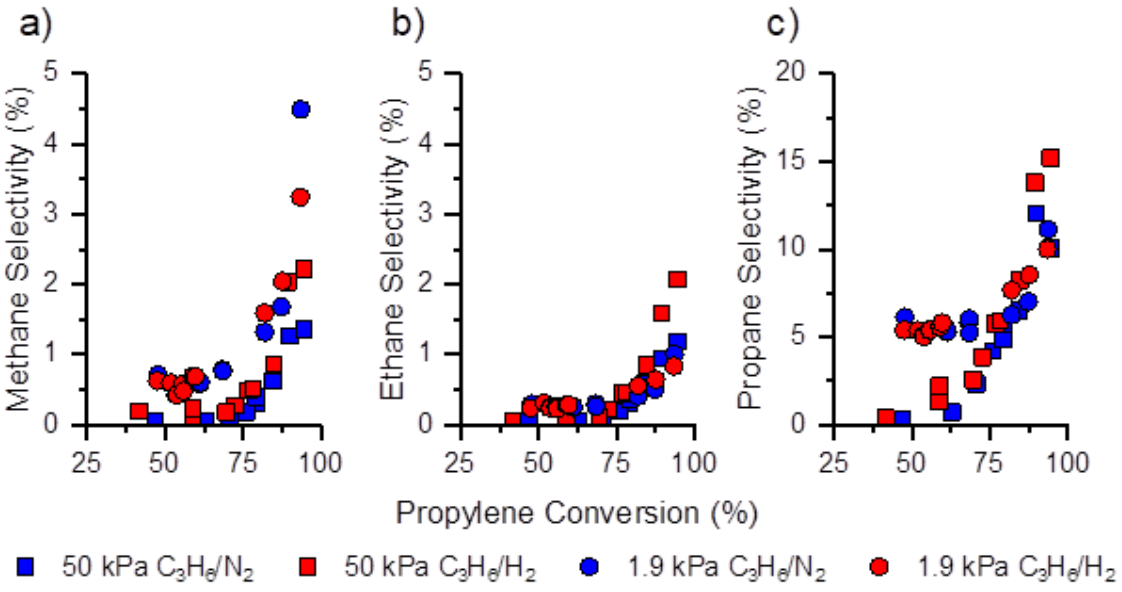

Figure 3.6. The carbon selectivity to a) methane, b) ethane, and c) propane as a function of propylene conversion in the presence and absence of 1.9 kPa H_2 on Ga/H-ZSM-5 at 723 K, 1.9 kPa C_3H_6, balance N_2.

At 1.9 kPa, the differences between co-feeding N_2 and H_2 disappear. Benzene (Figure 3.5a, blue circles), toluene (Figure 3.5b, blue circles), and xylene (Figure 3.5c, blue circles) selectivities increase from 5%, 15%, and 15%, respectively, at 48% conversion, to 20%, 23%, and 20%, respectively, at 94% conversion.

The selectivity to light alkanes (i.e., methane, ethane, and propane) have relatively constant (and low) selectivity until approximately 75% conversion, and then begin to increase slightly. At 1.9 kPa C_3H_6 (blue circles), methane (Figure 3.6a), ethane (Figure 3.6b), and propane (Figure 3.6c) selectivity is constant at ≈ 0.7%, ≈ 0.3%, and 5%, respectively, until approximately 75%

conversion, and then increase to 4%, 7%, and 11%, respectively. When co-feeding 1.9 kPa H_2 (red circles), the trends are equivalent to that when co-feeding 1.9 kPa N_2.

Ethylene selectivity (Figure 3.7a) at 1.9 kPa C_3H_6 (circles) is relatively constant (≈ 17%) until 70% conversion, and then decreases to 6% at 94% conversion. C_4 selectivity (Figure 3.7b) when feeding 1.9 kPa C_3H_6 (circles) is relatively constant from 47 – 70% conversion, and then decreases to 7% selectivity at 94% conversion. In 1.9 kPa C_3H_6, C_5 and C_6 selectivity (Figure 3.7b and c, respectively) have maximum selectivity at the lowest conversion measured, and steadily decrease to <1% selectivity as conversion approaches 100%. Selectivity to C_{7+} species (Figure 3.7e) at 1.9 kPa (circles) is relatively constant at 8% across the conversion range tested. All the trends at 1.9 kPa are equivalent when co-feeding H_2 and N_2.

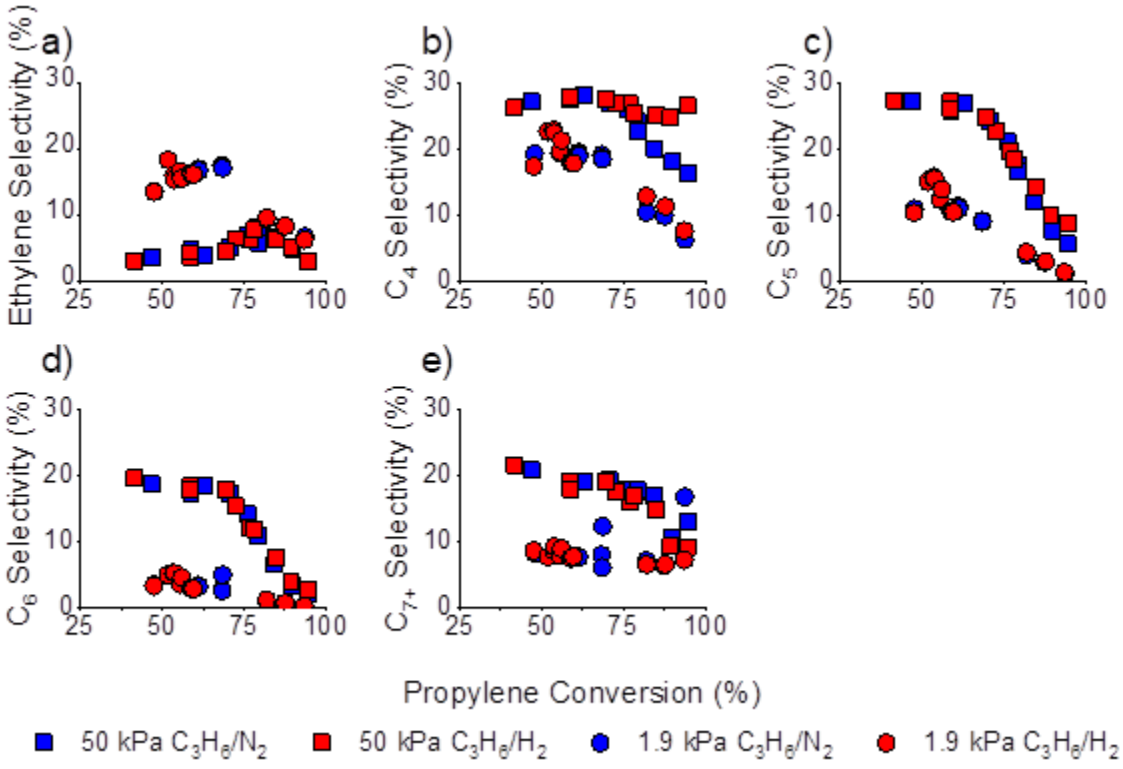

Figure 3.7. The carbon selectivity to a) ethene, b) butanes/enes (C_4), c) pentanes/enes (C_5), d) hexanes/enes (C_6), and e) larger non-aromatic hydrocarbons (C_{7+}) as a function of propylene conversion in the presence and absence of 1.9 kPa H_2 on Ga/H-ZSM-5 at 723 K, 1.9 kPa C_3H_6, balance N_2.

In summary, there were no significant differences in product distribution at 1.9 kPa C_3H_6 in the presence of H_2 on H-ZSM-5 or on Ga/H-ZSM-5 at 723 K. At 50 kPa C_3H_6, there are also no

differences in product selectivity on H-ZSM-5. For Ga/H-ZSM-5, there is also little difference at conversion below about 80%, but at higher conversions there is a small decrease in aromatic selectivity (approximately 3% decrease for benzene, toluene, and xylene, each) and an increased C_4 selectivity. Selectivities to the other products were unaffected by the presence of H_2.

3.4 Discussion

3.4.1 The Impact of H_2 on C_3H_6 Aromatization Product Distribution

The olefin product distributions in the presence and absence of H_2 were determined on H-ZSM-5. For H-ZSM-5, no differences in the product distribution were observed at either 1.9 kPa or 50 kPa. This suggests that H_2 does not substantially affect propylene aromatization on H-ZSM-5, indicating that Bronsted acid catalysts are ineffective dehydrogenation catalysts. These results are consistent with literature suggesting the formation of aromatics on Bronsted acid protons proceeds via cracking of larger hydrocarbons and subsequent isomerization of the double bond into the cyclic ring, forming alkanes as a by-product. The low selectivity to methane and ethane indicates that these alkanes are not significant by-products from the aromatization process but are rather formed via Bronsted acid cracking of alkanes at higher reaction temperatures.

On Ga/H-ZSM-5, there is also no difference in product distribution at 1.9 kPa (Figure 3.5 – Figure 3.7), thus suggesting that at low partial pressures H_2 does not impact propylene aromatization. Previous literature reports that there is an increased selectivity to BTX on Ga/H-ZSM-5 compared to H-ZSM-5, which is due to naphtha dehydrogenation on Ga. Thus, while it may be initially expected that co-feeding equimolar H_2 would suppress aromatics formation, this is not observed at 1.9 kPa. This may be due to Ga being an insufficiently active catalyst to inhibit aromatics formation. The low activity under these conditions is also supported by the similar selectivity observed to propane and ethane in the presence of co-fed H_2 (Figure 3.6b and c, respectively), i.e., reactant and product olefins are not hydrogenated. At lower pressures, thermodynamic equilibrium favors dehydrogenation products [51], thus reducing the thermodynamic driving force for hydrogenation compared to higher pressure. Because the thermodynamic equilibrium favors dehydrogenation compared to higher pressures across the entire range of conditions tested, Ga continues to dehydrogenate alkanes formed during aromatization, thus the presence of Ga allows for aromatization via dehydrogenation.

At 50 kPa C_3H_6 and H_2, decreased selectivity to toluene and xylene and increased selectivity to C_4 products at conversions >80% are observed. At conversions below 80%, product selectivities are indistinguishable in the presence and absence of H_2. The similar product distribution at conversions below 80% suggests that aromatization is occurring via dehydrogenation on Ga at these conversions. At high conversion (>80%), the selectivity to toluene and xylene decrease, while C_4 selectivity increases. The presence of excess H_2 at high conversions induces butene hydrogenation on Ga, resulting in the increased C_4 selectivity. Propylene and ethylene selectivity are unaffected by the co-fed H_2, indicating Ga is insufficiently active to hydrogenate the light olefins under these conditions. The reduced toluene and xylene selectivity are due to the rate of aromatic formation via dehydrogenation on Ga being reduced due to the buildup of excess H_2. At approximately 80% conversion, sufficient excess H_2 is present such that aromatization proceeds via cracking on H-ZSM-5. This interpretation is supported by the similar selectivity to toluene and xylene observed at 50 kPa while co-feeding H_2 on Ga/H-ZSM-5 and H-ZSM-5 (Figure 3.8a and b, respectively).

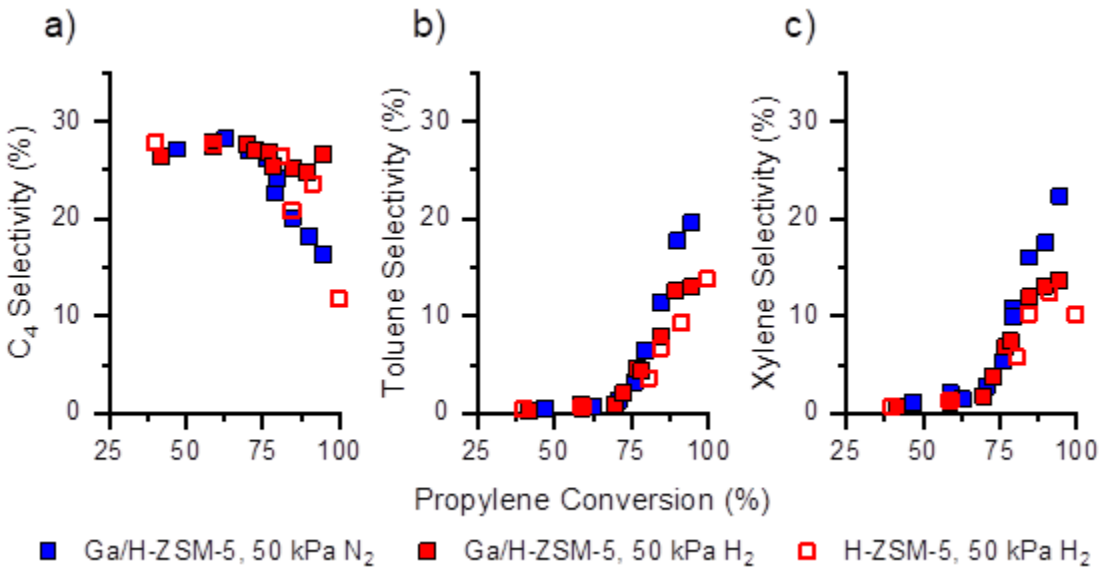

Figure 3.8. Comparison of a) C_4, b) toluene, and c) xylene selectivity as a function of conversion on H-ZSM-5 (unfilled) and Ga/H-ZSM-5 (filled). Reaction conditions: 50 kPa C_3H_6, 50 kPa H_2 or N_2, 723 K. Reproduced from Figure 3.1 and Figure 3.5.

3.4.2 The Impact of Ga on C_3H_6 Aromatization Product Distribution

By comparing the product distribution of Ga/H-ZSM-5 and H-ZSM-5 under equivalent conditions (i.e., isoconversion and in the same gas treatments), the effect of Ga on C_3H_6 aromatization can be ascertained. At 1.9 kPa, Ga/H-ZSM-5 has a higher selectivity to each aromatic than H-ZSM-5 (Figure 3.9), in agreement with previous reports that Ga increases selectivity to aromatics for olefin aromatization due to Ga enabling catalytic dehydrogenation of cyclic hydrocarbons [17,18,33,38,39]. On both Ga/H-ZSM-5 and H-ZSM-5, aromatic selectivity initially increases at around 45% conversion (Figure 3.9a), and similar aromatic selectivity is achieved at near complete propylene conversion. However, aromatic selectivity on Ga/H-ZSM-5 increases more significantly at lower conversions (i.e., 45% - 80%) compared to H-ZSM-5. At higher conversions (i.e., >80%), the aromatic selectivity increases more rapidly on H-ZSM-5, ultimately achieving a similar selectivity as near-complete conversion is achieved.

The increased selectivity on Ga/H-ZSM-5 is offset by a decreased selectivity to non-aromatic C_{4+} hydrocarbons (Figure 3.9b) and propane (Figure 3.9c) compared to H-ZSM-5. This is consistent with Ga dehydrogenating cyclic hydrocarbons, whereas H-ZSM-5 produces alkanes as a by-product of aromatics formation. Ga enabling catalytic dehydrogenation converts larger hydrocarbons into aromatic rings, resulting in a reduced selectivity to reactive intermediates, especially at intermediate conversions. The increased selectivity to propane on H-ZSM-5 compared to Ga/H-ZSM-5 suggests that Bronsted acid sites form propane during aromatization, whereas on Ga/H-ZSM-5, propane is formed to a lesser extent. Additionally, propane may be converted to propylene on Ga via catalytic dehydrogenation, thus reducing the selectivity on Ga/H-ZSM-5.

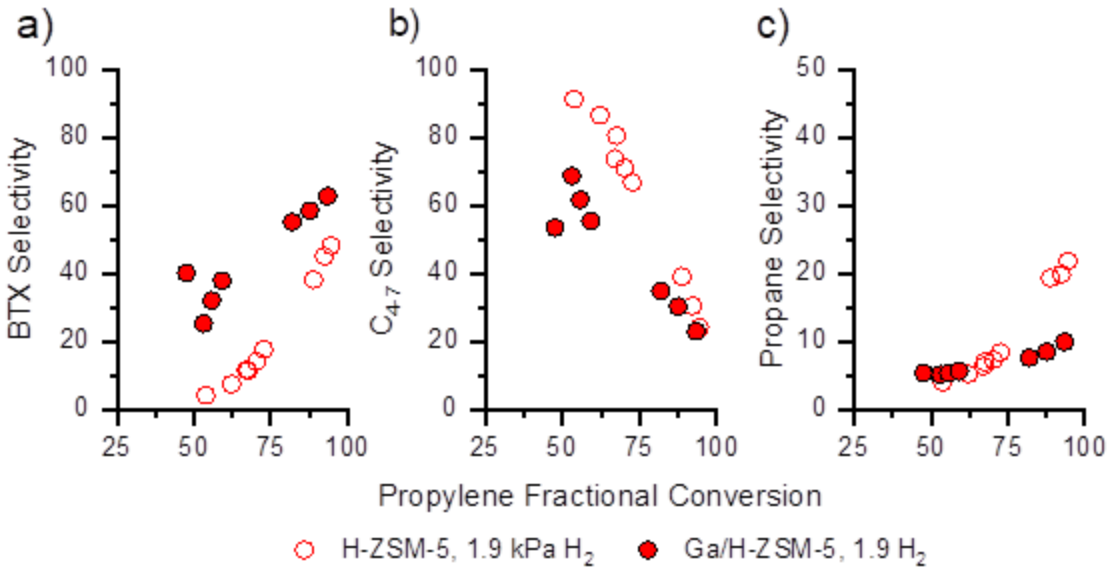

Figure 3.9. Comparison of a) combined aromatic (BTX), b) hydrocarbons with at least 4 carbons, and c) propane selectivities as a function of conversion on H-ZSM-5 (unfilled) and Ga/H-ZSM-5 (filled) in 1.9 kPa H_2, 1.9 kPa C_3H_6, balance N_2 at 723 K. Data reproduced from Figure 3.1 – Figure 3.7.

As mentioned above, at 50 kPa, the presence of H_2 affects the product distribution on Ga/H-ZSM-5 at conversions above 80%, thus Figure 3.10 and Figure 3.11 compare the product distributions in the absence and presence of H_2, respectively. Without H_2, the Ga/H-ZSM-5 demonstrates an increased selectivity to aromatics (Figure 3.10a) at conversions above 85%, and a lower selectivity to light alkanes (i.e., propane). However, at conversions below 85%, where most industrial processes are operated, the product distribution on Ga/H-ZSM-5 is equivalent to that of H-ZSM-5. When H_2 is present, as described above, the product distribution on Ga/H-ZSM-5 and H-ZSM-5 are equivalent (Figure 3.11). Thus, practically, Ga demonstrates no significant impact on the product distribution of propylene aromatization at 50 kPa, contrasting with the results observed at 1.9 kPa.

The observation that Ga/H-ZSM-5 does not impact aromatics selectivity at 50 kPa contrasts with previous conclusions that Ga/H-ZSM-5 increases the selectivity to aromatics compared to H-ZSM-5 [17,18,33,39]. However, previous studies examined propylene aromatization at different partial pressures of C_3H_6 [17,18,33,39], compared reaction products at equivalent space velocity as opposed to equivalent conversion [17,18,39], or both. As is evident in this study, the partial pressure of C_3H_6 shifts the product distribution trends on Ga/H-ZSM-5 and H-ZSM-5, and is

discussed further, below. Additionally, propylene is reformed via cracking reactions on Bronsted acid sites [32], thus space velocity is not analogous to conversion for aromatization reactions. For example, Shibata et al. compare H-ZSM-5 and Ga/H-ZSM-5 at equivalent contact time (W/F = 10.0 g h mol^{-1}) and achieve 80% on H-ZSM-5 but reach near-100% conversion on Ga/H-ZSM-5 [17].

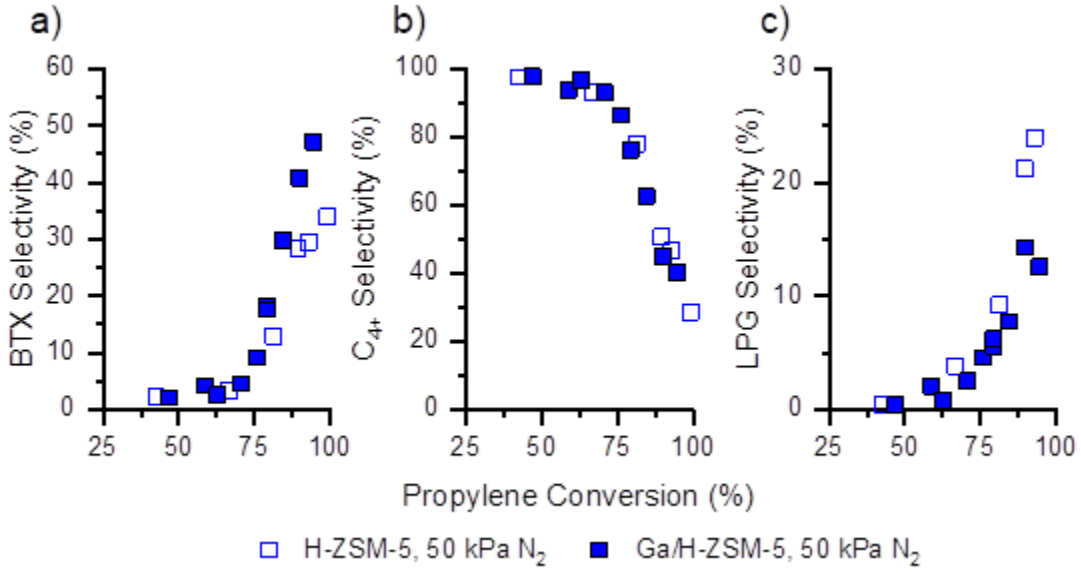

Figure 3.10. Comparison of a) combined BTX, b) hydrocarbons with at least 4 carbons, and c) combined light gas (i.e., methane, ethane, and propane selectivity as a function of conversion on H-ZSM-5 (unfilled) and Ga/H-ZSM-5 (filled) for C_3H_6 aromatization. Reaction conditions: 50 kPa C_3H_6, 50 kPa N_2, 723 K. Data reproduced from Figure 3.1 – Figure 3.7.

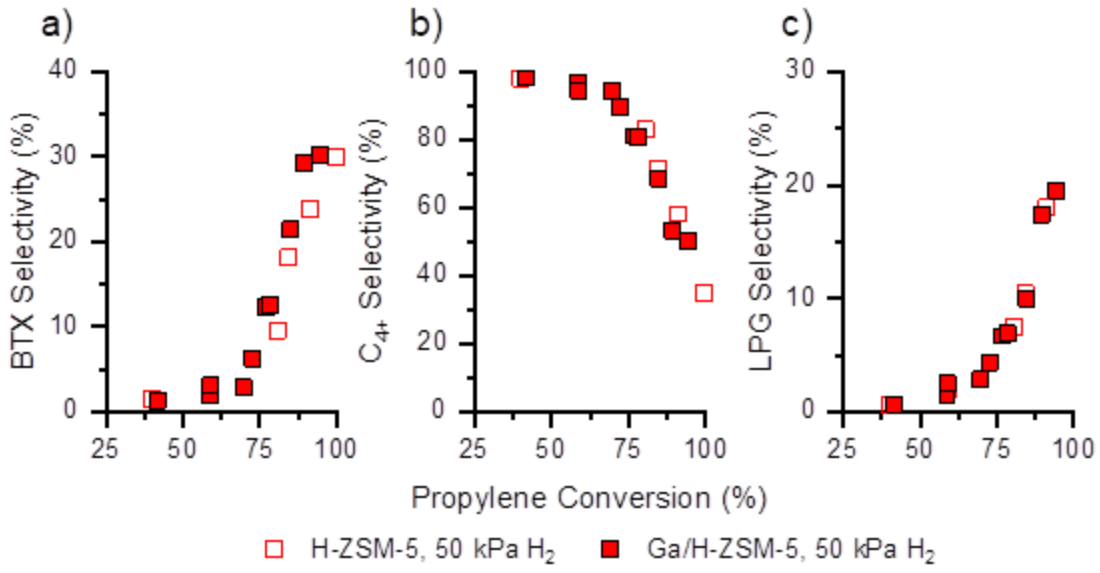

Figure 3.11. Comparison of a) combined BTX, b) hydrocarbons with at least 4 carbons, and c) combined light gas (i.e., methane, ethane, and propane selectivity as a function of conversion on H-ZSM-5 (unfilled) and Ga/H-ZSM-5 (filled) for C_3H_6 aromatization in H_2. Reaction conditions: 50 kPa C_3H_6, 50 kPa H_2, 723 K. Data reproduced from Figure 3.1 – Figure 3.7.

3.4.3 The Impact of C_3H_6 Partial Pressure on Aromatization Product Distribution

On both H-ZSM-5 (Figure 3.1 – Figure 3.3) and Ga/H-ZSM-5 (Figure 3.5 – Figure 3.7), increasing the partial pressure results in a shift in product distribution to form more heavy molecular weight, non-aromatic species and fewer aromatic and light alkane species. Methane and ethane selectivity are lower at 50 kPa than at 1.9 kPa (Figure 3.2 and Figure 3.6 for H-ZSM-5 and Ga/H-ZSM-5, respectively). At conversions below 80%, propane selectivity is lower at 50 kPa than at 1.9 kPa, however as conversion increases, propane selectivity increases more rapidly at 50 kPa, ultimately resulting in a higher selectivity at near complete propylene conversion. This is attributed to shifts in the equilibrium of olefin hydrogenation at higher pressures. Increasing the partial pressure of C_3H_6 and H_2 from 1.9 kPa to 50 kPa, an increase by a factor of 26, shifts the equilibrium of olefin hydrogenation to favor alkanes more significantly [51]. The presence of the Ga functionality has been broadly reported to increase aromatic selectivity by shifting the mechanism for aromatic formation to be catalytic dehydrogenation. The suppression of dehydrogenation due to shifting equilibrium may also be in part responsible for the decreased selectivity to aromatics (Figure 3.5) and increased selectivity to C_{4+} species at intermediate conversions (Figure 3.7b-e). As previously discussed, at 50 kPa C_3H_6 and H_2, C_4 selectivity on

Ga/H-ZSM-5 significantly increases at conversions above 80% due to the hydrogenation of C_4 olefins, consistent with the increase in partial pressure shifting the equilibrium towards hydrogenation products. However, due to the variety of isomers present in the higher molecular weight species, determining the relative degree of dehydrogenation was infeasible for this study.

3.5 Conclusions

By cross-comparing the product distribution of propylene aromatization in the presence and absence of 1.9 or 50 kPa C_3H_6 co-fed with H_2 or N_2 on Ga/H-ZSM-5 and H-ZSM-5, the effects of Ga, H_2, and pressure were observed. Ga was shown to enhance aromatic selectivity, especially at 1.9 kPa, through catalytic dehydrogenation enhancing rates of aromatization. At higher pressures, this effect is minimized as dehydrogenation equilibrium shifts to greater favor paraffinic products, thereby reducing the differences in aromatic selectivity on Ga compared to H^+. The presence of equimolar H_2, that which would be produced during dehydrogenation of alkanes prior to olefin aromatization that could be employed in a two-stage alkane dehydroaromatization process, was shown to have minimal impact on the product distribution of H-ZSM-5, suggesting that Bronsted acid protons are non-reactive for dehydrogenation during aromatization. On Ga/H-ZSM-5 at 1.9 kPa, the product selectivity is also unaffected, suggesting that Ga remains active for catalytic dehydrogenation at these conditions. At 50 kPa, where the dehydrogenation equilibrium favors alkanes more significantly, the product selectivity in the presence of equimolar H_2 shifts the product distribution on Ga/H-ZSM-5 to be equivalent to that of H-ZSM-5, corroborating the notion that Ga enhances aromatic selectivity via catalytic dehydrogenation of cyclic hydrocarbons to form aromatic rings. The effect of pressure on C_3H_6 aromatization served to increase the selectivity of heavy non-aromatic hydrocarbons regardless of the catalyst used or co-fed species. Discussion of the role of an intracrystalline organic phase and diffusion constraints resulting in this shift in the product distribution was incorporated.

4. CONCLUSIONS AND RECOMMENDATIONS

The work in this thesis is designed to evaluate the efficacy of a process for converting olefins to aromatics and high-octane gasoline. In the first study (Chapter 2), it was found that the product distribution as a function of conversion of all reactive species (i.e., the fed propylene and reactive molecules that would be recycled in a process) is independent of the inclusion of a dehydrogenation function, although the dehydrogenation function does increase aromatization rates. This suggests that including a dehydrogenation function is beneficial as a smaller reactor is necessary to achieve equivalent conversion. However, this also suggests that further enhancing aromatic selectivity requires changes in the acid function.

Additionally, the first study showed that increasing the temperature of the reaction increases the selectivity to aromatics; however, higher temperatures shift the product distribution to favor benzene over toluene and xylene. Thus, the process must be optimized considering both the total aromatic selectivity as well as the aromatic distribution. For example, for gasoline applications, benzene is limited due to environmental hazards; thus, the process would need to operate at lower temperatures to minimize benzene selectivity. However, at lower temperatures, the overall selectivity to aromatics is reduced. Thus, a greater understanding for the mechanism of formation of aromatics ring is necessary. As seen in the cyclohexene aromatization results, the most abundant aromatic formed on acid catalysts is xylene, suggesting that some intrinsic aspect of the mechanism forms xylenes.

As aforementioned, olefins that would be used to generate aromatics are derived from the conversion of alkanes, which simultaneously forms hydrogen. To develop this two-stage process, an understanding of the necessity of separating hydrogen between reaction steps is required. The second study showed that the presence of hydrogen has little impact on the product distribution on H-ZSM-5 and Ga/H-ZSM-5, suggesting that the hydrogen separation from light alkanes and olefins is not required, saving significant costs. Results also indicate that the partial pressure of the reactants has a significant impact on the product distribution. In particular, higher pressures eliminate the benefits that Ga exhibits on aromatic selectivity at equivalent propylene conversion. In order to develop this process, then, optimization of the reaction pressure that achieves the optimal product distribution while minimizing hydrogenation is one area that requires further investigation.

Based on these results, a variety of areas for further investigation are necessary further development of this process. Process optimization to determine the optimal catalyst, temperature, pressure, and conversion are necessary. As seen in Chapter 3, pressure has the largest impact on the product distribution. Increasing process pressure shifts the product distribution to favor higher molecular weight hydrocarbons (i.e., those with at least 4 carbons), and fewer aromatics at equivalent propylene conversion. This may be beneficial for processes making high octane gasoline rather than making aromatics. However, the aromatic distribution also needs to be balanced. For gasoline applications, benzene must be converted to alternative species, for example into ethylbenzene using the olefins present in the process. Changing the temperature also affects the product distribution. Increasing the temperature increases the production of aromatics by converting smaller alkanes. For example, at 723 K, propane and butane are not reactive, whereas at 823 K, they become reactive to form aromatics. However, at higher temperatures, the aromatic distribution shifts to generate more benzene and less toluene and xylene. Thus, further economic optimization of the process is necessary to balance these competing interests for the process.

Next, the choice of hydrogen separation must be optimized. Notably, the presence of hydrogen yields similar product distributions on H-ZSM-5, thus the pre-separation step is not necessary if using H-ZSM-5. However, removing the H_2 may increase the aromatic selectivity slightly at high conversions on Ga/H-ZSM-5, thus a partial H_2 separation may be desirable if the increase in aromatic selectivity is economically beneficial. Finally, the conversion must be optimized. If seeking gasoline, intermediate propylene conversion is acceptable, generating mostly olefins. However, if seeking to maximize aromatics, higher propylene conversion is necessary. Additionally, olefins that are not converted can be recycled to enhance aromatics formation. Process optimizations may be conducted as part of Thrust 4 within CISTAR.

Finally, further testing on the effects of hydrogen for catalyst stability and deactivation mechanisms will be important for developing this process. Recent reports suggest that the presence of hydrogen helps prevent coke formation on the surface of silica and alumina supports. The presence of excess hydrogen may also inhibit coke formation on H-ZSM-5 during aromatization, which would be beneficial for the development of olefin aromatization processes. Further studies of the impact of hydrogen on catalyst stability is another potential area of future study.

REFERENCES

1. Ridha T, Li Y, Gençer E, Siirola J, Miller J, Ribeiro F, et al. Valorization of Shale Gas Condensate to Liquid Hydrocarbons through Catalytic Dehydrogenation and Oligomerization. Processes. 2018;6(9):139.

2. Cybulskis VJ, Bukowski BC, Tseng HT, Gallagher JR, Wu Z, Wegener E, et al. Zinc Promotion of Platinum for Catalytic Light Alkane Dehydrogenation: Insights into Geometric and Electronic Effects. ACS Catal [Internet]. 2017;7(6):4173–81. Available from: https://pubs.acs.org/doi/abs/10.1021/acscatal.6b03603

3. Caspary KJ, Gehrke H, Heinritz-Adrian M, Schwefer M. Dehydrogenation of Alkanes. In: Handbook of Heterogeneous Catalysis: Online [Internet]. 2008. p. 3206–29. Available from: https://onlinelibrary.wiley.com/doi/epdf/10.1002/9783527610044.hetcat0162

4. Bricker JC. Advanced catalytic dehydrogenation technologies for production of olefins. Top Catal. 2012;55(19–20):1309–14.

5. Phadke NM, Mansoor E, Head-Gordon M, Bell AT. Mechanism and kinetics of light alkane dehydrogenation and cracking over isolated Ga species in Ga/H-MFI. ACS Catal. 2021;11(4):2062–75.

6. Krannila H, Haag WO, Gates BC. Monomolecular and bimolecular mechanisms of paraffin cracking: n-butane cracking catalyzed by HZSM-5. J Catal [Internet]. 1992;135(1):115–24. Available from: https://www.sciencedirect.com/science/article/pii/002195179290273K

7. Vora B V. Development of dehydrogenation catalysts and processes. Top Catal. 2012;55(19–20):1297–308.

8. Sundaram KM, Froment GF. Modeling of thermal cracking kinetics-I. Thermal cracking of ethane, propane and their mixtures. Chem Eng Sci. 1977;32(6):601–8.

9. Kotrel S, Knözinger H, Gates BC. The Haag-Dessau mechanism of protolytic cracking of alkanes. Microporous and Mesoporous Materials. 2000;35–36:11–20.

10. Lashchinskaya ZN, Gabrienko AA, Arzumanov SS, Kolganov AA, Toktarev A V, Freude D, et al. Which Species, Zn(II) Cations or ZnO Clusters , Are More Efficient for Olefin Aromatization? 13C Solid-State NMR Investigation of n-But-1-ene Transformation on Zn-Modified Zeolite. ACS Catal. 2020;10:14224–33.

11. Lukyanov DB, Gnep NS, Guisnet M. Kinetic Modeling of Ethene and Propene Aromatization over HZSM-5 and GaHZSM-5. Ind Eng Chem Res [Internet]. 1994;33(2):223–34. Available from: Lukyanov, D. B., Gnep, N. S. & Guisnet, M. R. Kinetic Modeling of Ethene and Propene Aromatization HZSM-5. Ind. Eng. Chem. Res 33, 223–234 (1994).

12. Su X, Fang Y, Gao P, Liu Y, Hou G, Bai X. In-situ microwave synthesis of nano-GaZSM-5 bifunctional catalysts with controllable location of active GaO+ species for olefins aromatization. Microporous and Mesoporous Materials [Internet]. 2020;306:1–10. Available from: https://doi.org/10.1016/j.micromeso.2020.110388

13. Choudhary VR, Kinage AK, Choudhary T V. Simultaneous aromatization of propane and higher alkanes or alkenes over H-GaAlMFI zeolite. Chemical Communications [Internet]. 1996;(22):2545–6. Available from: https://pubs.rsc.org/en/content/articlehtml/1996/cc/cc9960002545

14. Fegade SL, Tande BM, Cho H, Seames WS, Sakodynskaya I, Muggli DS, et al. Aromatization of Propylene Over Hzsm-5: a Design of Experiments (DOE) Approach. Chem Eng Commun. 2013;200(8):1039–56.

15. Ono Y. Transformation of Lower Alkanes into Aromatic Hydrocarbons over ZSM-5 Zeolites. Catalysis Reviews [Internet]. 1992;34(3):179–226. Available from: https://www.tandfonline.com/doi/abs/10.1080/01614949208020306

16. Lechert H, Bezouhanova C, Dimitrov C, Nenova V. Intermeditaes in the formation of aromatics from propene and 2-propanol on H-ZSM-5 zeolites. Zeolites as Catalysts, Sorbents and Detergent Builders. 1989;91–8.

17. Shibata M, Kitagawa H, Sendoda Y, Ono Y. Transformation of propene into aromatic hydrocarbons over ZSM-5 zeolites. Stud Surf Sci Catal. 1986;28(C):717–24.

18. Ono Y, Kitagawa H, Sendoda Y. Transformation of But-1-ene into Aromatic Hydrocarbons Over ZSM-5 Zeolites. Journal of Chemical Society, Faraday Transactions. 1987;83(9):2913–23.

19. Biscardi A, Iglesia E. Structure and function of metal cations in light alkane reactions. Catal Today [Internet]. 1996;31:207–31. Available from: https://www.sciencedirect.com/science/article/pii/S0920586196000284

20. Nayak VS, Choudhary VR. Selective poisoning of stronger acid sites on HZSM-5 in the conversion of alcohols and olefins to aromatics. Appl Catal. 1984;9:251–61.

21. Le Van Mao R, Dufresne LA, Yao J, Yu Y. Effects of the nature of coke on the activity and stability of the hybrid catalyst used in the aromatization of ethylene and n-butane. Appl Catal A Gen. 1997;164(1–2):81–9.

22. Arishtirova K, Dimitrov Chr, Dyrek K, Hallmeier KHz, Popova Z, Witkowski S. Influences of copper on physico-chemical and catalytic properties of ZSM-5 zeolites in the reaction of ethene aromatization. Appl Catal A Gen. 1992;81(1):15–26.

23. Norval GW, Phillips MJ, Virk KS, Simons R V. Olefin conversion over zeolite H-ZSM-5. Can J Chem Eng. 1989;67(3):521–3.

24. Poutsma ML. Mechanistic Considerations of Hydrocarbon Transformations Catalyzed by Zeolites. In: Rabo JA, editor. Zeolite Chemistry and Catalysis. Washington, D.C.: American Chemical Society; 1976. p. 437–521.

25. Huang M, Kaliaguine S. Propene aromatization over alkali-exchanged ZSM-5 zeolites. Journal of Molecular Catalysis. 1993;81(1):37–49.

26. Popova Z, Aristirova K, Dimitrov Chr. Aromatization of propene on ZSM-5 zeolites. Reaction Kinetics & Catalysis Letters. 1990;41(2):369–74.

27. Saito H, Sekine Y. Catalytic conversion of ethane to valuable products through non-oxidative dehydrogenation and dehydroaromatization. RSC Adv. 2020;10(36):21427–53.

28. Han SW, Park H, Han J, Kim J chul, Lee J, Jo C, et al. PtZn Intermetallic Compound Nanoparticles in Mesoporous Zeolite Exhibiting High Catalyst Durability for Propane Dehydrogenation. ACS Catal. 2021;11:9233–41.

29. Chang CW, Pham HN, Alcala R, Datye AK, Miller JT. Dehydroaromatization Pathway of Propane on PtZn/SiO2+ ZSM-5 Bifunctional Catalyst. ACS Sustain Chem Eng. 2022;10(1):394–409.

30. Fiuza TER, Zanchet D. Supported AuCu Alloy Nanoparticles for the Preferential Oxidation of CO (CO-PROX). ACS Appl Nano Mater. 2020;3(1):923–34.

31. Meriaudeau P, Sapaly G, Naccache C. On the Role of Ga, Pt, PtCu, and PtGa in HZSM-5 for the Cyclisation of Propane into Aromatics. In: Jacobs PA, van Santen RA, editors. Studies in Surface Science and Catalysis. Elsevier; 1989. p. 1423–9.

32. Santilli DS. Mechanism of Hexane Cracking in ZSM-5. Appl Catal. 1990;60:137–41.

33. Qiu P, Lunsford JH, Rosynek MP. Characterization of Ga/ZSM-5 for the catalytic aromatization of dilute ethylene streams. Catal Letters. 1998;52(1):37–42.

34. Nozik D, Bell AT. Role of Ga3+Sites in Ethene Oligomerization over Ga/H-MFI. ACS Catal. 2022;12(22):14173–84.

35. Zhou Y, Thirumalai H, Smith SK, Whitmire KH, Liu J, Frenkel AI, et al. Ethylene Dehydroaromatization over Ga-ZSM-5 Catalysts: Nature and Role of Gallium Speciation. Angewandte Chemie. 2020;132(44):19760–9.

36. Nagamori Y, Kawase M. Converting light hydrocarbons containing olefins to aromatics (Alpha Process). Microporous and Mesoporous Materials. 1998;21(4–6):439–45.

37. Pidko EA, Hensen EJM, Santen RAV. Anionic oligomerization of ethylene over Ga/ZSM-5 zeolite: A theoretical study. Journal of Physical Chemistry C. 2008;112(49):19604–11.

38. Bhan A, Delgass WN. Propane aromatization over HZSM-5 and Ga/HZSM-5 catalysts. Catal Rev Sci Eng [Internet]. 2008;50(1):19–151. Available from: Bhan, A. & Delgass, W. N. Propane Aromatization over HZSM-5 and Ga/HZSM-5 Catalysts. Catal. Rev. 19–151 (2008). doi:10.1080/01614940701804745

39. Choudhary VR, Panjala D, Banerjee S. Aromatization of propene and n-butene over H-galloaluminosilicate (ZSM-5 type) zeolite. Appl Catal A Gen [Internet]. 2002;231(1–2):243–51. Available from: https://www.sciencedirect.com/science/article/pii/S0926860X02000613

40. Chen NY, Yan TY. M2 forming a process for aromatization of light hydrocarbons. Industrial and Engineering Chemistry Process Design and Development. 1986;25(1):151–5.

41. Epsilon Software. Almelo, The Netherlands: Malvern Panalytical B.V.; 2019.

42. Epsilon Dashboard. Almelo, The Netherlands: Malvern Panalytical B.V.; 2019.

43. Getsoian AB, Das U, Camacho-Bunquin J, Zhang G, Gallagher JR, Hu B, et al. Organometallic model complexes elucidate the active gallium species in alkane dehydrogenation catalysts based on ligand effects in Ga K-edge XANES. Catal Sci Technol. 2016;6(16):6339–53.

44. Higby PL, Shelby JE, Phillips JC, Legrand AD. EXAFS study of alkali galliosilicate glasses. J Non Cryst Solids. 1988;105(1–2):139–48.

45. Behrens P, Kosslick H, Vu Anh Tuan, Fröba M, Neissendorfer F. X-ray absorption spectroscopic study on the structure and crystallization of Ga-containing MFI-type zeolites. Microporous Materials. 1995;3(4–5):433–41.

46. Nishi K, Shimizu KI, Takamatsu M, Yoshida H, Satsuma A, Tanaka T, et al. Deconvolution analysis of Ga K-Edge XANES for quantification of gallium coordinations in oxide environments. Journal of Physical Chemistry B. 1998;102(50):10190–5.

47. LiBretto NJ, Xu Y, Quigley A, Edwards E, Nargund R, Vega-Vila JC, et al. Olefin oligomerization by main group Ga3+ and Zn2+ single site catalysts on SiO2. Nat Commun. 2021;12(1):1–9.

48. Phadke NM, Van Der Mynsbrugge J, Mansoor E, Getsoian AB, Head-Gordon M, Bell AT. Characterization of Isolated Ga3+ Cations in Ga/H-MFI Prepared by Vapor-Phase Exchange of H-MFI Zeolite with GaCl3. ACS Catal. 2018;8(7):6106–26.

49. Xu Y, Libretto NJ, Zhang G, Miller JT, Greeley J. First-Principles Analysis of Ethylene Oligomerization on Single-Site Ga3+Catalysts Supported on Amorphous Silica. ACS Catal. 2022;12(9):5416–24.

50. Cybulskis VJ, Pradhan SU, Lovón-Quintana JJ, Hock AS, Hu B, Zhang G, et al. The Nature of the Isolated Gallium Active Center for Propane Dehydrogenation on Ga/SiO2. Catal Letters. 2017;147(5):1252–62.

51. Sattler JJHB, Ruiz-Martinez J, Santillan-Jimenez E, Weckhuysen BM. Catalytic dehydrogenation of light alkanes on metals and metal oxides. Chem Rev. 2014;114(20):10613–53.

PUBLICATIONS

1. Russell, C. K.; Saxena, A.; Miller, J. T. Impact of PtZn nanoparticles on propylene aromatization on H-ZSM-5. Cat. Res. 2023; (*Under Review*).

2. Russell, C. K.; Rockey, J.; Hanna, R.; & Miller, J. T. Impact of Co-Fed Hydrogen on High Conversion Propylene Aromatization on H-ZSM-5 and Ga/H-ZSM-5. Cat. Res. 2023; (*In Preparation*).

3. Miller JT, LiBretto NJ, Russell CK, Conrad MA. Zinc(II) and Gallium(III) catalysts for olefin reactions. 17/109,515, 2021. p. 1–16.

4. Dean DP, Leshchev L, Stavitski E, Deshmukh G, Russell CK, Zhu K, Miller JT. Valence-to-core X-ray emission spectroscopy to resolve the size dependent valence electronic structure of Pt nanoparticles. ACS Catal. 2023; (*In Preparation*)

5. Lardinois TM, Bates JS, Lippie HH, Russell CK, Miller JT, Meyer HM, et al. Structural Interconversion between Agglomerated Palladium Domains and Mononuclear Pd(II) Cations in Chabazite Zeolites. Chem Mater. 2021;33(5):1698–713.

6. Yuda A, Kumar A, Abu Reesh I, Russell CK, Miller JT, Ali Saleh Saad M, et al. Electrooxidation of methanol on Ag, AgNi, and AgCo catalysts prepared by combustion synthesis technique. Int J Energy Res. 2022;46(15):22162–75.

7. Qi L, Zhang Y, Conrad MA, Russell CK, Miller J, Bell AT. Ethanol Conversion to Butadiene over Isolated Zinc and Yttrium Sites Grafted onto Dealuminated Beta Zeolite. J Am Chem Soc. 2020;142(34):14674–87.

8. Bolton, B., et al. Mechanistic Insights into the Hysteresis Phenomena during NH_3 Oxidation on Pt/Al2O3 Catalysts for NH3 Slip Applications. 2023; (*In Preparation*)